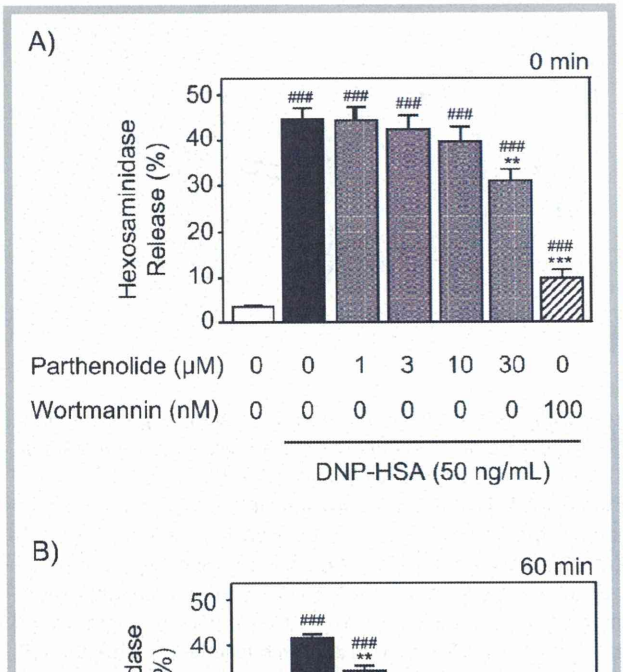

Fig. 2 Effects of parthenolide on antigen-induced degranulation. **A** IgE-sensitized RBL-2H3 cells were incubated for 20 min in PIPES buffer containing DNP-HSA (50 ng/mL) and the indicated concentration of parthenolide. **B** IgE-sensitized RBL-2H3 cells were preincubated for 60 min in medium containing the indicated concentration of parthenolide. The cells were further incubated for 20 min in PIPES buffer containing DNP-HSA (50 ng/mL) and the corresponding concentration of parthenolide. Values are the means for four samples with the SEM shown by vertical bars. Statistical significance: ### $p < 0.001$ vs. the unstimulated control, ** $p < 0.01$, *** $p < 0.001$ vs. the stimulated control.

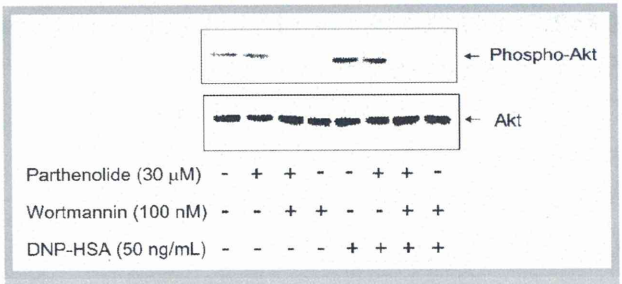

Fig. 3 Effects of parthenolide on the antigen-induced phosphorylation of Akt. IgE-sensitized RBL-2H3 cells were preincubated for 60 min with (+) or without (−) parthenolide (30 μM) or wortmannin (100 nM). The cells were further incubated for 15 min in PIPES buffer containing DNP-HSA (50 ng/mL) and the corresponding concentration of parthenolide or wortmannin. The levels of phospho-Akt and Akt were determined by Western blotting. Similar results were obtained in three separate sets of experiments.

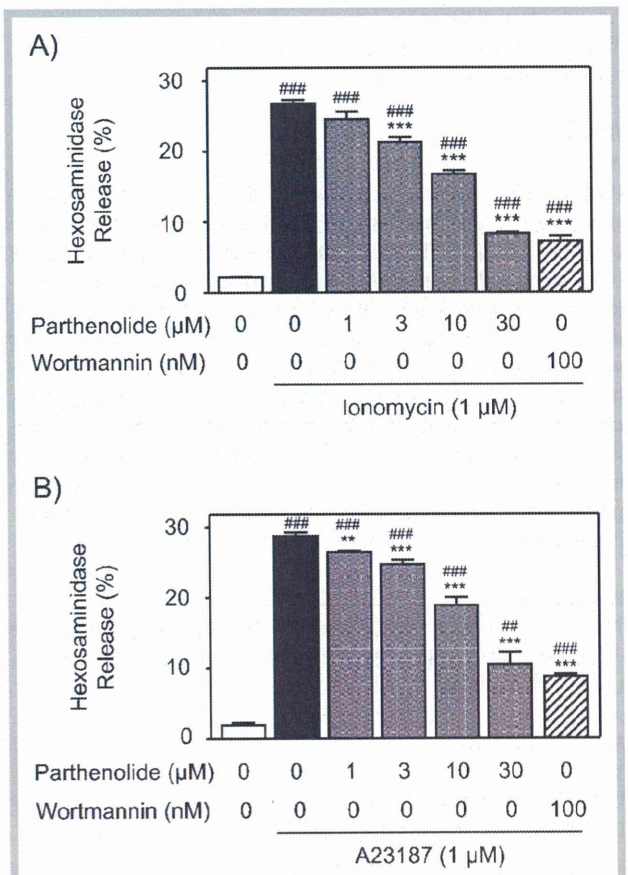

Fig. 4 Effects of parthenolide on ionomycin- and A23187-induced degranulation. RBL-2H3 cells were preincubated for 60 min in medium containing the indicated concentration of parthenolide or wortmannin. The cells were further incubated for 15 min in PIPES buffer containing ionomycin (1 μM) (**A**), or A23187 (1 μM) (**B**), and the corresponding concentration of parthenolide or wortmannin. Values are the means for four samples with the SEM shown by vertical bars. Statistical significance: ## $p < 0.01$, ### $p < 0.001$ vs. the unstimulated control, * $p < 0.05$, ** $p < 0.01$, *** $p < 0.001$ vs. the stimulated control.

pressed the antigen-induced increase in $[Ca^{2+}]i$ levels in a concentration-dependent manner (**Fig. 5C** to **F**). These findings suggested that parthenolide suppressed the antigen-induced increase in $[Ca^{2+}]i$ levels, thereby inhibiting antigen-induced degranulation. Wortmannin (100 nM) also suppressed the increase in $[Ca^{2+}]i$ levels almost completely (data not shown). To further confirm that parthenolide inhibits an increase in $[Ca^{2+}]i$ levels, changes in $[Ca^{2+}]i$ levels over time in randomly selected adherent cells on the surface of glass-bottomed dishes were examined with a confocal laser scanning microscope. The antigen stimulation increased the level of $[Ca^{2+}]i$ in each adherent cell (**Fig. 6A**), but treatment with parthenolide (30 μM) almost completely suppressed the antigen-induced increase in $[Ca^{2+}]i$ levels (**Fig. 6B**). Treatment with wortmannin (100 nM) had the same effect (**Fig. 6C**). The calcium ionophore ionomycin (1 μM) also in-

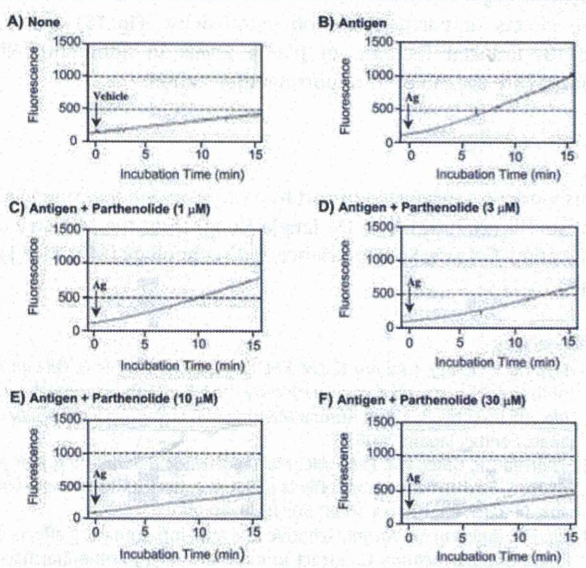

Fig. 5 Effects of parthenolide on the antigen-induced increase in $[Ca^{2+}]i$ levels in suspended cells. The IgE-sensitized cells were preincubated for 60 min in medium containing various concentrations of parthenolide (**C** to **F**), scraped off the wells, and suspended in medium. The cells were then loaded with Fura-2 AM and stimulated with DNP-HSA (50 ng/mL), and $[Ca^{2+}]i$ levels were determined with a fluorescence spectrometer in the presence of parthenolide. An arrow indicates when the antigen (Ag) was added.

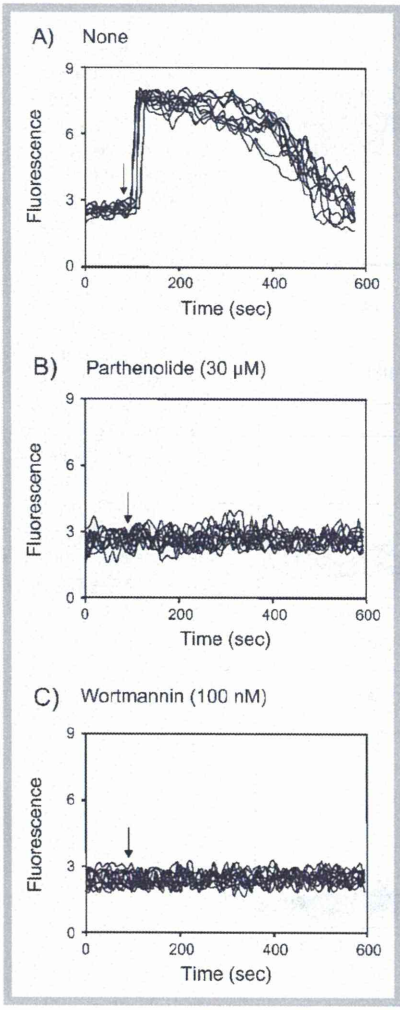

Fig. 6 Effects of parthenolide on the antigen-induced increase in $[Ca^{2+}]i$ levels in adherent cells. The IgE-sensitized cells were preincubated for 60 min in medium containing no agent (**A**), parthenolide (30 μM) (**B**), or wortmannin (100 nM) (**C**). The cells were then loaded with Fura-2 AM and stimulated with DNP-HSA (50 ng/mL). $[Ca^{2+}]i$ levels in each cell (10 cells) were determined with a confocal laser scanning microscope in the presence of each drug. An arrow indicates when the antigen was added.

creased $[Ca^{2+}]i$ levels. Treatment with parthenolide (30 μM) or wortmannin (100 nM) suppressed the ionomycin-induced increase in $[Ca^{2+}]i$ levels (**Fig. 7A**), but the early phase increase was partially retained (**Fig. 7B** and **C**). It was also observed in the case of A23187 (1 μM) (**Fig. 2S**). Different from the result of the antigen stimulation, the ionomycin-induced degranulation was not completely inhibited by parthenolide (30 μM) (**Fig. 4A**). This might be due to the finding that parthenolide (30 μM) did not completely inhibit the early phase increase in $[Ca^{2+}]i$ levels (**Fig. 7B** and **C**).

Parthenolide has been shown to inhibit NF-κB [10]. In addition, it inhibited p38 mitogen-activated protein kinase (MAPK) in human monocyte-derived dendritic cells [11], and p42/44 MAPK in rat primary microglial cells [12]. It was reported that inositol 1,4,5-trisphosphate produced by the PI3K pathway triggers an increase in $[Ca^{2+}]i$ [13]. Our finding that parthenolide did not suppress the PI3K pathway (**Fig. 3**) but inhibited the antigen-induced increase in the level of $[Ca^{2+}]i$ (**Fig. 5** and **6**) suggested that it acts on a pathway other than that of PI3K.

Recently, Miyata et al. [14] reported that parthenolide inhibited the mast cell degranulation induced by an antigen but had little effect on that triggered by a calcium ionophore. The discrepancy might be due to the different conditions used for the preincubation with parthenolide. They also reported that parthenolide inhibited mast cell degranulation by preventing microtubule formation [14]. We indicated that parthenolide suppressed both antigen-induced and calcium ionophore-induced degranulation by inhibiting an increase in the level of $[Ca^{2+}]i$. As it was reported that an increase in cytosolic calcium maintains the plasma membrane's integrity through the formation of a microtubule ring [15], it is possible that the reduction by parthenolide of $[Ca^{2+}]i$ levels contributed to the decrease in microtubule formation. Further study is necessary to clarify the mechanism by which parthenolide inhibits an increase in the level of $[Ca^{2+}]i$ without interfering with the PI3K pathway.

Parthenolide prevents degranulation of mast cells by inhibiting an increase in the level of $[Ca^{2+}]i$. This inhibitory effect should also be examined in human mast cells because there is a species-dependent difference between these and rodent mast cells [16].

Materials and Methods

The culturing of rat basophilic leukemia RBL-2H3 cells (Health Science Research Resources Bank) and sensitization with dinitrophenol-specific IgE were performed according to methods described previously [17]. The sensitized cells were incubated for a specified period in medium containing the antigen DNP-HSA (50 ng/mL) in the presence or absence of parthenolide (purity: ≥ 97%; Wako). The cells were also activated by ionomycin (1 μM; purity: ≥ 98%; Calbiochem) or A23187 (1 μM; purity: ≥ 98%; Calbiochem). The drugs were dissolved in dimethylsulfoxide (DMSO) and added to the buffer. The final concentration of DMSO was adjusted to 0.1% (v/v) in all groups. As a positive control, the PI3K inhibitor wortmannin (purity: ≥ 98%; Sigma) was used.

Cytotoxicity was determined by using 3-(4,5-dimethylthiazol-2-yl)-2,5-diphenyltetrazolium bromide (MTT; Sigma) [17]. As an index of degranulation, the level of hexosaminidase activity in

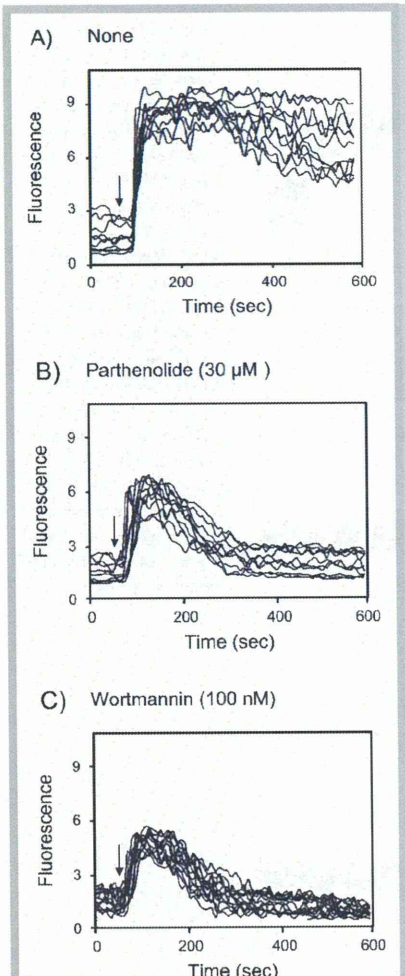

Fig. 7 Effects of parthenolide on the ionomycin-induced increase in $[Ca^{2+}]i$ levels in adherent cells. The IgE-sensitized cells were preincubated for 60 min in medium containing no agent (**A**), parthenolide (30 μM) (**B**), or wortmannin (100 nM) (**C**). The cells were then loaded with Fura-2 AM and stimulated with ionomycin (1 μM). $[Ca^{2+}]i$ levels in each cell (10 cells) were determined with a confocal laser scanning microscope in the presence of each drug. An arrow indicates when ionomycin was added.

the buffer 20 min after the stimulation and in the cells were determined as described [17]. Phosphorylation of Akt was determined after separation by sodium dodecylsufate-polyacrylamide gel (8%) electrophoresis (125 V, 2 h), by Western blotting using a polyclonal antibody for phospho-Akt (Ser473; Cell Signaling Technology). After heating for 30 min at 60 °C in stripping buffer (60 mM Tris-HCl, pH 6.7, 70 mM sodium dodecylsufate, and 0.7% [v/v] 2-mercaptoethanol), Akt was reblotted with Akt antibody (Cell Signaling Technology) [17].

$[Ca^{2+}]i$ levels were determined with a fluorescence spectrometer (F-2000, Hitachi) in cells scraped off the wells, loaded with Fura-2 AM (Wako), and stimulated with DNP-HSA (50 ng/mL). To examine changes in $[Ca^{2+}]i$ levels in each cell, adherent cells on the surface of the glass-based dishes (Iwaki) were loaded with Fura-2 AM, and stimulated with the antigen. The changes in $[Ca^{2+}]i$ levels in randomly selected cells were determined with a confocal laser scanning microscope (Fluoview FV 100, FV10-ASW, Olympus).

Percent of hexosaminidase released is expressed as the means ± SEM for four wells in one set of experiments. The statistical analysis of the results obtained was made with Dunnett's test. The results were confirmed with at least three independent sets of experiments.

Supporting information

The effects of parthenolide on cytotoxicity (**Fig. 1S**) and on A23187-induced increase in $[Ca^{2+}]i$ levels in adherent cells (**Fig. 2S**) are available as Supporting Information.

Acknowledgements

This work was supported in part by a Grant-in-Aid for Young Scientists (B) (20790214; to Dr. JangJa Hong) from the Ministry of Education, Culture, Sports, Science and Technology (MEXT) of Japan.

References

1 *Aoyama S, Hong J, Ishihara K, Lee XM, Oh JS, Kwak JH, Zee O, Ohuchi K.* Inhibition of mast cell degranulation by the NF-κB inhibitor parthenolide. Abstract No. 3, 126th Annual Meeting of Pharmaceutical Society of Japan, Sendai, Japan; 2006: 5

2 *Schinella GR, Giner RM, Recio MC, Mordujovich de Buschiazzo P, Ríos JL, Máñez S.* Anti-inflammatory effects of South American *Tanacetum vulgare*. J Pharm Pharmacol 1998; 50: 1069–1074

3 *Jain NK, Kulkarni SK.* Antinociceptive and anti-inflammatory effects of *Tanacetum parthenium* L. extract in mice and rats. J Ethnopharmacol 1999; 68: 251–259

4 *Felteistein ME, Schühlkly W, Warnick JE, Fischer NH, Sufka KJ.* Anti-inflammatory and anti-hyperalgesic effects of sesquiterpene lactones from Magnolia and Bear's foot. Pharmacol Biochem Behav 2004; 79: 299–302

5 *López-Franco O, Suzuki Y, Sanjuán G, Blanco J, Hernández-Vargas P, Yo Y, Kopp J, Egido J, Gómez-Guerrero C.* Nuclear factor-κB inhibitors as potential novel anti-inflammatory agents for the treatment of immune glomerulonephritis. Am J Pathol 2002; 161: 1497–1505

6 *Tournier H, Schinella G, de Balsa EM, Buschiazzo H, Mañez S, Mordujovich de Buschiazzo P.* Effect of the chloroform extract of *Tanacetum vulgare* and one of its active principles, parthenolide, on experimental gastric ulcer in rats. J Pharm Pharmacol 1999; 51: 215–219

7 *Reuter U, Chiarugi A, Bolay H, Moskowitz MA.* Nuclear factor-κB as a molecular target for migraine therapy. Ann Neurol 2002; 51: 507–516

8 *Zingarelli B, Hake PW, Denenberg A, Wong HR.* Sesquiterpene lactone parthenolide, an inhibitor of IκB kinase complex and nuclear factor-κB, exerts beneficial effects in myocardial reperfusion injury. Shock 2002; 17: 127–134

9 *Kiuchi H, Takao T, Yamamoto K, Nakayama J, Miyagawa Y, Tsujimura A, Nonomura N, Okuyama A.* Sesquiterpene lactone parthenolide ameliorates bladder inflammation and bladder overactivity in cyclophosphamide induced rat cystitis model by inhibiting nuclear factor-κB phosphorylation. J Urol 2009; 181: 1987–1988

10 *Hehner SP, Hofmann TG, Dröge W, Schmitz ML.* The antiinflammatory sesquiterpene lactone parthenolide inhibits NF-κB by targeting the IκB kinase complex. J Immunol 1999; 163: 5617–5623

11 *Uchi H, Arrighi JF, Aubry JP, Furue M, Hauser C.* The sesquiterpene lactone parthenolide inhibits LPS- but not TNF-α -induced maturation of human monocyte-derived dendritic cells by inhibition of the p38 mitogen-activated protein kinase pathway. J Allergy Clin Immunol 2002; 110: 269–276

12 *Fiebich BL, Lieb K, Engels S, Heinrich M.* Inhibition of LPS-induced p42/44 MAP kinase activation and iNOS/NO synthesis by parthenolide in rat primary microglial cells. J Neuroimmunol 2002; 132: 18–24

13 *Ching TT, Hsu AL, Johnson AJ, Chen CS.* Phosphoinositide 3-kinase facilitates antigen-stimulated Ca^{2+} influx in RBL-2H3 mast cells via a phosphatidylinositol 3,4,5-trisphosphate-sensitive Ca^{2+}entry mechanism. J Biol Chem 2001; 276: 14814–14820

14 *Miyata N, Gon Y, Nunomura S, Endo D, Yamashita K, Matsumoto K, Hashimoto S, Ra C.* Inhibitory effects of parthenolide on antigen-induced microtubule formation and degranulation in mast cells. Int Immunopharmacol 2008; 8: 874–880

15 *Wang P, Xu S, Zhao K, Xiao B, Guo J.* Increase in cytosolic calcium maintains plasma membrane integrity through the formation of microtubule ring structure in apoptotic cervical cancer cells induced by trichostatin. Cell Biol Int 2009; 33: 1149–1154

16 *Bischoff SC.* Role of mast cells in allergic and non-allergic immune responses: comparison of human and murine data. Nat Rev Immunol 2007; 7: 93–104
17 *Hong J, Sasaki H, Hirasawa N, Ishihara K, Kwak JH, Zee O, Schmitz FJ, Seyama T, Ohuchi K.* Suppression of the antigen-stimulated RBL-2H3 mast cell activation by artekeiskeanol A. Planta Med 2009; 75: 1494–1498

received January 26, 2010
revised June 30, 2010
accepted July 7, 2010

Bibliography
DOI http://dx.doi.org/10.1055/s-0030-1250221
Published online September 2, 2010
Planta Med 2011; 77: 252–256

ISSN 0032-0943

Correspondence
JangJa Hong, PhD
Laboratory of Life Sciences
Faculty of Pharmacy
Yasuda Women's University
6-13-1 Yasuhigashi
Asaminami-ku
731-0153 Hiroshima
Japan
Phone: + 81 8 28 78 94 51
Fax: + 81 8 28 78 28 96
ohuchi-k@mail.pharm.tohoku.ac.jp

Drug Metab. Pharmacokinet. 26 (5): 544–547 (2011).

SNP Communication

Novel Single Nucleotide Polymorphism of the *CYP2A13* Gene in Japanese Individuals

Yuichiro Tamaki[1], Masashi Honda[1], Yuka Muroi[1], Tomio Arai[2], Haruhiko Sugimura[3], Yoichi Matsubara[4], Shuichi Kanno[5], Masaaki Ishikawa[5], Noriyasu Hirasawa[1] and Masahiro Hiratsuka[1,*]

[1]*Laboratory of Pharmacotherapy of Life-Style Related Diseases, Graduate School of Pharmaceutical Sciences, Tohoku University, Sendai, Japan*

[2]*Department of Pathology, Tokyo Metropolitan Geriatric Hospital, Tokyo, Japan*

[3]*Department of Pathology 1, Hamamatsu University School of Medicine, Hamamatsu, Japan*

[4]*Department of Medical Genetics, Tohoku University School of Medicine, Sendai, Japan*

[5]*Department of Clinical Pharmacotherapeutics, Tohoku Pharmaceutical University, Sendai, Japan*

Full text of this paper is available at http://www.jstage.jst.go.jp/browse/dmpk

Summary: Cytochrome P450 2A13 (CYP2A13) is a human CYP enzyme that is selectively expressed in the respiratory tract. It plays an active role in the metabolic activation of a tobacco-specific procarcinogen. In this study, the entire coding sequence and the exon-intron junctions of the *CYP2A13* gene obtained from 395 Japanese individuals were screened for genetic polymorphisms. Eight genetic polymorphisms were found, of which seven gave rise to known variant alleles: CYP2A13*2, CYP2A13*3, CYP2A13*4, CYP2A13*6, and CYP2A13*7. We identified a novel single nucleotide polymorphism (SNP), 5792T>C, in exon 7 that caused an amino acid substitution (Ile331Thr). One of the 395 individuals included in the study was heterozygous for the variant allele, and therefore, the frequency of the allele in the study population was 0.13%.

Keywords: CYP2A13; genetic polymorphism; SNP; Japanese

Introduction

Cytochrome P450s (CYPs) play an important role in the metabolism of a variety of compounds, including therapeutic agents, environmental toxicants, and chemical carcinogens. CYP2A13 is selectively expressed in the human respiratory tract; the highest level of expression is observed in the nasal mucosa, followed by the tracheal mucosa, and finally the lungs.[1–5] CYP2A13 plays an active role in the metabolism of many xenobiotic compounds such as 4-(methylnitrosamino)-1-(3-pyridyl)-1-butanone (NNK), which is a major tobacco-specific procarcinogen, and *N*-nitrosomethylphenylamine and is also involved in the detoxification of carcinogens including *N*,*N*-dimethylaniline.[3] Therefore, CYP2A13 may play an important role in xenobiotic toxicity and tobacco-related carcinogenesis in the respiratory tract and lungs.

The *CYP2A13* gene is located in a *CYP* gene cluster on chromosome 19.[6] To date, nine alleles of *CYP2A13* have been identified (*CYP2A13*1–9*).[7–9] Genetic variations affecting CYP2A13 enzyme function may lead to interindividual variability in susceptibility to diseases, including lung cancer. In the present study, we screened nine exons and exon-intron junctions of the *CYP2A13* gene from 395 Japanese individuals for genetic polymorphisms by using denaturing high-performance liquid chromatography (DHPLC). We identified one novel single nucleotide polymorphism (SNP) of the *CYP2A13* gene among the Japanese individuals included in the study; this novel polymorphism was nonsynonymous.

Received; April 17, 2011, Accepted; May 7, 2011

J-STAGE Advance Published Date: May 24, 2011, doi:10.2133/dmpk.DMPK-11-SC-033

**To whom correspondence should be addressed:* Masahiro Hiratsuka, Ph.D., *Laboratory of Pharmacotherapy of Life-Style Related Diseases, Graduate School of Pharmaceutical Sciences, Tohoku University, 6-3 Aoba, Aramaki, Aoba-ku, Sendai 980-8578, Japan. Tel. +81-22-717-7049, Fax. +81-22-717-7049, E-mail: mhira@m.tohoku.ac.jp*

On March 7, 2011, the variation was not found in the Japanese Single Nucleotide Polymorphism (JSNP) (http://snp.ims.u-tokyo.ac.jp/) database, the National Center for Biotechnology Information (http://www.ncbi.nlm.nih.gov/SNP/), the Human CYP Allele Nomenclature Committee (http://www.cypalleles.ki.se/) database, or the PharmGKB (http://www.pharmgkb.org/) database. The *CYP2A13* haplotype with 74G>A, 3375C>T, and 5792T>C was assigned as *CYP2A13*10* by the Human CYP Allele Nomenclature Committee.

This work was supported by a grant from the Smoking Research Foundation and in part by KAKENHI (20590154) from the Japan Society for the Promotion of Science (JSPS).

Table 1. Amplification and DHPLC conditions for *CYP2A13* SNP analysis of genomic DNA

Exon	Size (bp)	Forward primer (5′-3′)	Reverse primer (5′-3′)	Annealing temp. (°C)	PCR cycles	DHPLC temp. (°C)
1–5[1]	4,817	GCTACACACTCCACCTCCCAGAAACTCCAC	AGGTGTGTCTGCTAACCAGGACATGAACGG	68	25	—
1[2]	257	AACCACCCCAGCCATCACCA	CCCACCCCGTGCCACCC	60	25	60.8, 62.8
2[2]	244	GGGGGCTGCTCCCTCTAACCA	ATCCACCTGGCCACCTTCCC	60	25	61.2, 64.2
3[2]	236	CGCCCCCTGACCTCTCTCCA	AGAAAGCGCGGGTTCCCG	60	25	64.0
4[2]	241	TGACTCTCTCCCCAACCCCCTTC	GTTGTGGTAGGGGCGTCACTGG	60	25	61.6, 62.6
5[2]	260	TGACAGCTGTCCTTCCCTTCCCA	CCTGGCTTTGCACCTGCCTG	60	25	59.7, 61.7
6–9[1]	3,528	CCCTAGCTCAAACCCTGGTCTCTCTGAGCC	TTCCTCTCATCACAGCTCCTGAAGGACATC	65	25	—
6[2]	230	AAGAGCATGGAGAGTGAGCTTGGTCT	GAGGGTCTGGGGCCCTTCACTT	60	25	60.3, 62.3
7[2]	286	CATCCCTGCTCTAAGACCCCTAGACAC	GAAGTCCCCGTAGTCTGAGTGGTGG	60	25	58.5, 60.5
8[2]	224	CCCCCAACCTGCCTCATTACACA	TGTGAGCCGTGGCCTGGC	60	25	59.4, 60.4
9[2]	271	GAGAGTGGGCTTCACCTTCACCC	GTTTCCCTGGCCCCGCC	60	25	59.8, 61.8, 63.8

[1]First-round PCR. [2]Second-round PCR.

Materials and Methods

Human DNA samples: In the present study, DNA samples were obtained at the autopsies of 395 diseased patients in the Department of Pathology, Tokyo Metropolitan Geriatric Hospital, Tokyo, Japan, and were analyzed. The research protocols were approved by the Ethics Committees of the Tokyo Metropolitan Geriatric Hospital and the Graduate School of Pharmaceutical Sciences, Tohoku University.

Polymerase chain reaction (PCR) and DHPLC conditions: The primer pairs used to amplify the nine exons and the exon-intron junctions of the *CYP2A13* gene are listed in **Table 1**. These primers were designed on the basis of a genomic sequence reported in GenBank (NG_000008.7). The first-round long PCR was performed to specifically amplify exons 1–5 and 6–9 of the *CYP2A13* gene. Genomic DNA (10–50 ng) was amplified using LA-Taq DNA polymerase (TaKaRa, Otsu, Japan). The PCR thermal profile consisted of an initial denaturation at 95°C for 1 min; followed by 25 repetitive cycles of denaturation at 95°C for 15 s, annealing at 68°C or 65°C for 20 s, and extension at 72°C for 5 min; and then a final extension at 72°C for 7 min.

The first-round PCR products were diluted 1:500 in water and used as DNA templates for the second round of PCR for amplification of all the *CYP2A13* exons. The amplicons for each exon were generated using AmpliTaq Gold PCR Master Mix (Applied Biosystems, Foster City, CA, USA). PCR for the second round comprised an initial denaturation at 95°C for 10 min; followed by 25 repetitive cycles of denaturation at 95°C for 30 s, annealing at 60°C for 30 s, and extension at 72°C for 30 s; and then a final extension at 72°C for 7 min. Heteroduplexes were generated by thermal cycling under the following conditions: 95°C for 1 min, followed by 45 temperature decrements of 1.5°C/min.

The PCR products were analyzed using the DHPLC system WAVE (Transgenomic Inc., Omaha, NE, USA). Amplified PCR samples (5 μL) were separated on a heated C18 reverse-phase column by using 0.1 M triethylammonium acetate (TEAA) in water and 0.1 M TEAA in 25% acetonitrile at a flow rate of 0.9 mL/min. We determined the temperature for heteroduplex separation of a heterozygous *CYP2A13* fragment using the software that was provided with the DHPLC system. The DHPLC running conditions for each amplicon are summarized in **Table 1**. The linear acetonitrile gradient was adjusted so that the retention time of the DNA peak was 3–5 min. The resultant chromatograms were compared with those of the wild-type DNA. We sequenced both strands of samples in which variants were detected using DHPLC.

To determine the linkage among the polymorphisms identified in this study, we amplified long fragments of DNA obtained from the individuals who were heterozygous for both the SNPs by using PCR. The fragments were run on gels, purified using columns, and then ligated to a pCR-XL-TOPO vector (Invitrogen Co., CA, USA). The ligation products was transfected into *Escherichia coli*, and single colonies (each containing a plasmid with only one of the two alleles) were collected and the plasmids were isolated, after which the plasmid DNA was sequenced.

Results and Discussion

We found a novel SNP during this study and provide its details below. SNP: 110224Hiratsuka013; GENE NAME: *CYP2A13*; ACCESSION NUMBER: NG_000008; LENGTH: 25 bases; SEQUENCE: 5′-TCCATGAGGAGAT/CTGACAGAGTGAT-3′.

DHPLC analysis showed that exons 1, 2, 3, 5, 7, and 9 in the *CYP2A13* gene obtained from the 395 DNA samples had distinct chromatographic profiles from those of the wild-type DNA. We tested the specificity of DHPLC for detecting the variant allele in these exons by comparing the

Table 2. Detected SNPs of the *CYP2A13* gene in DNA samples of 395 Japanese individuals

Nucleotide change	Location	Predicted amino acid change	Frequency (%)
74G>A	Exon 1	R25Q	5.57
578C>T	Exon 2	R101X	0.38
579G>A	Exon 2	R101Q	0.13
1634_1635insACC	Exon 3	133_134insT	1.77
1706C>G	Exon 3	D158E	1.77
3375C>T	Exon 5	R257C	5.57
5792T>C	Exon 7	I331T	0.13
7465C>T	Exon 9	R494C	0.25

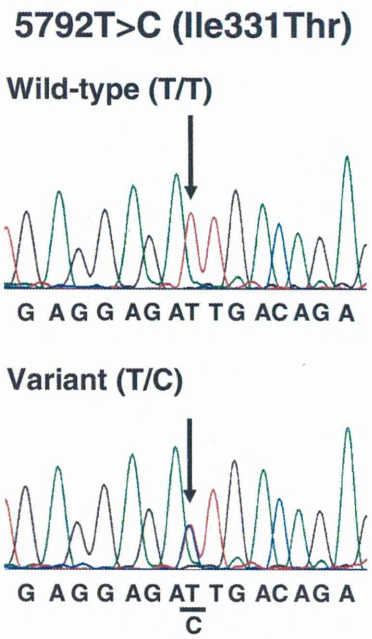

Fig. 1. Nucleotide sequences of the *CYP2A13* gene in exon 7
Although the sequences of only the sense strands are shown here, both strands were sequenced. Arrows indicate the variant nucleotide positions.

results of DHPLC with those of direct sequencing. Eight SNPs (74G>A, 578C>T, 579G>A, 1634_1635insACC, 1706C>G, 3375C>T, 5792T>C, and 7465C>T), including one novel SNP, were detected in the DNA samples of the Japanese individuals included in the study (**Table 2**). The novel SNP was 5792T>C in exon 7 (**Fig. 1**), and it resulted in an amino acid change of Ile331Thr. Experimental haplotype analysis by long PCR, cloning, and DNA sequencing showed that three SNPs, 74G>A, 3375C>T, and 5792T>C, exist in the same allele of the *CYP2A13* gene (data not shown). One of the 395 individuals was heterozygous for the novel SNP, and therefore, the frequency of the allele in the study population was 0.13%. The allele carrying the 74G>A, 3375C>T, and 5792T>C SNPs has been designated *CYP2A13*10*. The allele frequencies of *CYP2A13*1* (wild type), **2* (74G>A and 3375C>T), **3* (1634_1635insACC and 1706C>G), **4* (579G>A), **5* (7343T>A), **6* (7465C>T), **7* (578C>T), **8* (1706C>G), and **9* (5294G>T) were 0.916, 0.054, 0.018, 0.001, 0.000, 0.003, 0.004, 0.000, and 0.000, respectively. The sequence of each sample was confirmed by conducting at least two different PCR amplifications.

The novel SNP 5792T>C is located in exon 7 of the *CYP2A13* gene and results in an amino acid substitution, Ile331Thr. Smith *et al.* determined the crystalline structure of CYP2A13,[10] thus making it possible to predict precise locations of amino acid substitution within the three-dimensional structure. Ile331 is located at the start of the J-helix of CYP2A13.[11] Although this amino acid residue is not located on substrate recognition sites, it is known to be highly conserved in the CYP2 family in mammals. Therefore, the Ile331Thr substitution is expected to alter the catalytic properties of CYP2A13. Further studies are required to elucidate the functional characteristics of the novel variant allele of the *CYP2A13* gene.

In conclusion, we identified a novel nonsynonymous SNP in the *CYP2A13* gene in Japanese individuals. This nonsynonymous SNP was 5792T>C in exon 7, and it resulted in an amino acid substitution, Ile331Thr. In addition, the allele containing the 74G>A, 3375C>T, and 5792T>C SNPs has been designated *CYP2A13*10*.

References

1) Koskela, S., Hakkola, J., Hukkanen, J., Pelkonen, O., Sorri, M., Saranen, A., Anttila, S., Fernandez-Salguero, P., Gonzalez, F. and Raunio, H.: Expression of CYP2A genes in human liver and extrahepatic tissues. *Biochem. Pharmacol.*, **57**: 1407–1413 (1999).
2) Gu, J., Su, T., Chen, Y., Zhang, Q. Y. and Ding, X.: Expression of biotransformation enzymes in human fetal olfactory mucosa: potential roles in developmental toxicity. *Toxicol. Appl. Pharmacol.*, **165**: 158–162 (2000).
3) Su, T., Bao, Z., Zhang, Q. Y., Smith, T. J., Hong, J. Y. and Ding, X.: Human cytochrome P450 CYP2A13: predominant expression in the respiratory tract and its high-efficiency metabolic activation of a tobacco-specific carcinogen, 4-(methylnitrosamino)-1-(3-pyridyl)-1-butanone. *Cancer Res.*, **60**: 5074–5079 (2000).
4) Chen, Y., Liu, Y. Q., Su, T., Ren, X., Shi, L., Liu, D., Gu, J., Zhang, Q. Y. and Ding, X.: Immunoblot analysis and immunohistochemical characterization of CYP2A expression in human olfactory mucosa. *Biochem. Pharmacol.*, **66**: 1245–1251 (2003).
5) Ding, X. and Kaminsky, L. S.: Human extrahepatic cytochromes P450: function in xenobiotic metabolism and tissue-selective chemical toxicity in the respiratory and gastrointestinal tracts. *Annu. Rev. Pharmacol. Toxicol.*, **43**: 149–173 (2003).
6) Fernandez-Salguero, P., Hoffman, S. M., Cholerton, S., Mohrenweiser, H., Raunio, H., Rautio, A., Pelkonen, O., Huang, J. D., Evans, W. E., Idle, J. R. and Gonzalez, F. J.: A genetic polymorphism in coumarin 7-hydroxylation: sequence of the human CYP2A genes and identification of variant CYP2A6 alleles. *Am. J. Hum. Genet.*, **57**: 651–660 (1995).
7) Fujieda, M., Yamazaki, H., Kiyotani, K., Muroi, A., Kunitoh, H., Dosaka-Akita, H., Sawamura, Y. and Kamataki, T.: Eighteen novel polymorphisms of the CYP2A13 gene in Japanese. *Drug Metab. Pharmacokinet.*, **18**: 86–90 (2003).

8) Zhang, X., Chen, Y., Liu, Y., Ren, X., Zhang, Q. Y., Caggana, M. and Ding, X.: Single nucleotide polymorphisms of the human CYP2A13 gene: evidence for a null allele. *Drug Metab. Dispos.*, **31**: 1081–1085 (2003).
9) Cauffiez, C., Lo-Guidice, J. M., Quaranta, S., Allorge, D., Chevalier, D., Cenee, S., Hamdan, R., Lhermitte, M., Lafitte, J. J., Libersa, C., Colombel, J. F., Stucker, I. and Broly, F.: Genetic polymorphism of the human cytochrome CYP2A13 in a French population: implication in lung cancer susceptibility. *Biochem. Biophys. Res. Commun.*, **317**: 662–669 (2004).
10) Smith, B. D., Sanders, J. L., Porubsky, P. R., Lushington, G. H., Stout, C. D. and Scott, E. E.: Structure of the human lung cytochrome P450 2A13. *J. Biol. Chem.*, **282**: 17306–17313 (2007).
11) Lewis, D. F.: The CYP2 family: models, mutants and interactions. *Xenobiotica*, **28**: 617–661 (1998).

Drug Metab. Pharmacokinet. 26 (5): 516–522 (2011).

Regular Article

Association between Cancer Risk and Drug-metabolizing Enzyme Gene (*CYP2A6*, *CYP2A13*, *CYP4B1*, *SULT1A1*, *GSTM1*, and *GSTT1*) Polymorphisms in Cases of Lung Cancer in Japan

Yuichiro TAMAKI[1], Tomio ARAI[2], Haruhiko SUGIMURA[3], Takamitsu SASAKI[4], Masashi HONDA[1], Yuka MUROI[1], Yoichi MATSUBARA[5], Shuichi KANNO[6], Masaaki ISHIKAWA[6], Noriyasu HIRASAWA[1] and Masahiro HIRATSUKA[1,*]

[1]*Laboratory of Pharmacotherapy of Life-Style Related Diseases, Graduate School of Pharmaceutical Sciences, Tohoku University, Sendai, Japan*
[2]*Department of Pathology, Tokyo Metropolitan Geriatric Hospital and Institute of Gerontology, Tokyo, Japan*
[3]*First Department of Pathology, Hamamatsu University School of Medicine, Hamamatsu, Japan*
[4]*Department of Environmental and Health Science, Tohoku Pharmaceutical University, Sendai, Japan*
[5]*Department of Medical Genetics, Tohoku University School of Medicine, Sendai, Japan*
[6]*Department of Clinical Pharmacotherapeutics, Tohoku Pharmaceutical University, Sendai, Japan*

Full text of this paper is available at http://www.jstage.jst.go.jp/browse/dmpk

Summary: Genetic polymorphisms of enzymes involved in the metabolism of carcinogens are suggested to modify an individual's susceptibility to lung cancer. The purpose of this study was to investigate the relationship between lung cancer cases in Japan and variant alleles of cytochrome P450 (CYP) 2A6 (*CYP2A6*4*), CYP2A13 (*CYP2A13*1-*10*), CYP4B1 (*CYP4B1*1-*7*), sulfotransferase 1A1 (*SULT1A1*2*), glutathione *S*-transferase M1 (*GSTM1* null), and glutathione *S*-transferase T1 (*GSTT1* null). We investigated the distribution of these polymorphisms in 192 lung cancer patients and in 203 age- and sex-matched cancer-free controls. The polymorphisms were analyzed using various techniques including allele-specific PCR, hybridization probe assay, multiplex PCR, denaturing high-performance liquid chromatography (DHPLC), and direct sequencing. We also investigated allele and genotype frequencies and their association with lung cancer risk, demographic factors, and smoking status. The prevalence of the *CYP2A6*4/*4* genotype in lung cancer cases was 3.6%, compared with 9.4% in the controls (adjusted OR = 0.36, 95% CI = 0.15–0.88, $P = 0.025$). In contrast, there was no association between the known *CYP2A13*, *CYP4B1*, *SULT1A1*, *GSTM1*, and *GSTT1* polymorphisms and lung cancer. These data indicate that *CYP2A6* deletions may be associated with lung cancer in the Japanese population studied.

Keywords: lung cancer; CYP2A6; CYP2A13; CYP4B1; SULT1A1; GSTM1; GSTT1; genetic polymorphism

Introduction

Lung cancer is a major cause of cancer-related death worldwide.[1)] In Japan, lung cancer is the most common cause of death in the male population and the second most common cause of death in the female population, after colon cancer. Identifying the risk factors for lung cancer development is essential to prevent this deadly disease. Environmental exposure to tobacco smoke is the primary risk factor for lung cancer.[2,3)] Tobacco smoke contains hundreds of known and probable carcinogens that are either activated or detoxified by xenobiotic metabolizing enzymes. In general, the metabolism of xenobiotics consists of phases I and II. Phase I enzymes, mainly cytochrome P450 (CYP), are typically involved in metabolic pathways involving activation of carcinogens, whereas phase II enzymes play a central role in detoxification.

Received; May 25, 2011, Accepted; June 21, 2011
J-STAGE Advance Published Date: July 26, 2011, doi:10.2133/dmpk.DMPK-11-RG-046
**To whom correspondence should be addressed:* Masahiro HIRATSUKA, Ph.D., *Laboratory of Pharmacotherapy of Life-Style Related Diseases, Graduate School of Pharmaceutical Sciences, Tohoku University, 6-3 Aoba, Aramaki, Aoba-ku, Sendai 980-8578, Japan. Tel. +81-22-717-7049, Fax. +81-22-717-7049, E-mail: mhira@m.tohoku.ac.jp*
This work was supported by a grant from the Smoking Research Foundation, Japan.

Human CYP2A6 and CYP2A13 are important phase I enzymes involved in metabolizing nicotine and the metabolic activation of tobacco-specific nitrosamines such as 4-(methylnitrosamino)-1-(3-pyridyl)-1-butanone (NNK).[4,5] CYP2A6 is mainly expressed in the human liver, whereas CYP2A13 is selectively expressed in the human respiratory tract.[5,6] To date, a large number of *CYP2A6* and *CYP2A13* genetic polymorphisms and alleles have been identified (http://www.cypalleles.ki.se/). These alleles are derived from single nucleotide polymorphisms (SNPs) in regulatory and coding regions, deletions, insertions, and conversions. *CYP2A6*4* is a major mutant allele associated with decreased metabolic activity.[7] Several studies have elucidated the role of the *CYP2A6*4* allele in tobacco dependence and lung cancer risk.[8–10] Similarly, the *CYP2A13* polymorphism 3375C>T has been correlated with a reduced risk of lung adenocarcinoma in a Chinese population.[11]

CYP4B1 is primarily an extrahepatic form of P450. CYP4B1 mRNA has been detected in the human lung and bladder.[12,13] In animals, CYP4B1 is involved in the metabolism of several xenobiotics such as 2-aminofluorene, 2-naphthylamine, and benzidine.[14,15] To date, seven variant alleles of *CYP4B1* have been identified in French Caucasian and Japanese individuals. We previously reported that the alleles *CYP4B1*2* (AT881–882del, 993G>A, 1018C>T, and 1123C>T) and *CYP4B1*3* (517C>T) are common in the Japanese population.[16] In particular, premature termination of protein synthesis by the double nucleotide deletion AT881–882del has been speculated to render the *CYP4B1*2* allele non-functional. *CYP4B1* genotypes may have an effect on the risk of bladder cancer;[17] however, it is unclear whether *CYP4B1* polymorphisms are associated with lung cancer susceptibility.

Sulfotransferases (SULTs) appear to play an important role in phase II metabolism of xenobiotics, small endogenous compounds, and procarcinogenic agents.[18,19] Some studies have shown that genetic polymorphisms of *SULT1A1* are associated with susceptibility to lung cancer.[20,21]

Glutathione *S*-transferases (GSTs) are phase II enzymes that catalyze the conjugation of reactive intermediates to soluble glutathione. Some GSTs are polymorphic, and some genetic variants, such as *GSTM1* null and *GSTT1* null, may be associated with increased susceptibility to lung cancer.[22,23] Homozygous deletions of the *GSTM1* and *GSTT1* genes are common and result in complete loss of enzyme activity.

We conducted a case-control study to examine the association between the risk of lung cancer in Japanese individuals and P450s CYP2A6 (*CYP2A6*4*), CYP2A13 (*CYP2A13*1-*10*), CYP4B1 (*CYP4B1*1-*7*), sulfotransferase 1A1 (*SULT1A1*2*), glutathione *S*-transferase M1 (*GSTM1* null), and glutathione *S*-transferase T1 (*GSTT1* null) polymorphisms. In addition, we investigated the effect of smoking status and genetic combinations on the association between lung cancer risk and genetic polymorphisms.

Materials and Methods

Subject selection: From February 1995 to July 2003, 1,536 autopsies were performed at the Department of Pathology, Tokyo Metropolitan Geriatric Medical Center, Tokyo, Japan. DNA samples from 395 of these autopsies were analyzed in this case-control study; 192 lung cancer cases and 203 cancer-free controls were sex- and age-matched. The smoking status of the individuals was retrospectively determined by reviewing medical records, and subjects were classified as smokers (including current smokers and ex-smokers) and non-smokers (individuals who have never smoked in their lifetime). Research protocols were approved by the Ethics Committees of Tokyo Metropolitan Geriatric Hospital and the Graduate School of Pharmaceutical Sciences, Tohoku University.

Genetic analysis: The presence of *CYP2A6*4* (whole gene deletion) was determined by the two-step allele-specific PCR assay described by Oscarson *et al.*[24] The first step involved amplification of a region from exon 7 to approximately 420 bp downstream of exon 9 of *CYP2A6* or the *CYP2A6/CYP2A7* hybrid from all individuals with or without the deleted *CYP2A6* gene. The reaction mixture contained approximately 30 ng genomic DNA, 0.5 μM of each primer (2AE7F, 5′-GGCCAAGATGCCCTACATG-3′; 2A6R1, 5′-GCACTTATGTTTTGTGAGACATCAGAGACAA-3′), 0.25 mM dNTPs, LA Taq polymerase (TaKaRa, Otsu, Japan), and 2× GC Buffer I (TaKaRa) in a total reaction volume of 16 μL. The thermal cycling conditions were as follows: 95°C for 1 min; followed by 30 cycles of denaturation at 95°C for 15 s, annealing at 60°C for 20 s, extension at 72°C for 3 min; and a final extension at 72°C for 7 min. The PCR product was then used as a template in the second step, in which the deleted *CYP2A6* gene was detected. PCR amplification was performed with 0.5 μL of the first PCR product, 0.25 μM forward primer (2A6E8F, 5′-CACTTCCTGAATGAG-3′, or 2A7E8F, 5′-CATTTCCTGGATGAC-3′), 0.25 μM reverse primer (2A6R2, 5′-AAAATGGGCATGAACGCCC-3′), and 2× Amplitaq Gold PCR Master Mix (Applied Biosystems, Foster City, CA, USA) in a total volume of 20 μL. Thermal cycling conditions involved an initial denaturation at 95°C for 10 min; followed by 16 cycles of denaturation at 95°C for 30 s, annealing at 56°C for 30 s, extension at 72°C for 2 min; and a final extension at 72°C for 7 min. Amplified products were analyzed by electrophoresis in 1% agarose gel. The presence of a *CYP2A*-specific 1181-bp product amplified with the 2A6E8F/2A6R2 primer pair indicated the presence of wild-type *CYP2A6* (defined as *CYP2A6 non*4* allele in this study). The product amplified from the primer pair 2A7E8F/2A6R2 indicated a *CYP2A6* deletion (*CYP2A6*4*), and the presence of the product in both reactions from one individual indicated heterozygosity.

CYP2A13 genotypes were determined by our previously described assay.[25] Long PCR was performed in the first

round to amplify exons 1–5 and 6–9 of the *CYP2A13* gene using 10–50 ng of genomic DNA and LA-Taq DNA polymerase (TaKaRa). The thermal cycling consisted of an initial denaturation at 95°C for 1 min; followed by 25 cycles of denaturation at 95°C for 15 s, annealing at 68°C or 65°C for 20 s, and extension at 72°C for 5 min; and then a final extension at 72°C for 7 min. First-round PCR products were diluted 1:500 and used as templates for the second round of amplification for all *CYP2A13* exons. The amplicons for each exon were generated using AmpliTaq Gold PCR Master Mix (Applied Biosystems). Second-round PCR comprised an initial denaturation at 95°C for 10 min; followed by 25 cycles at 95°C for 30 s, annealing at 60°C for 30 s, and extension at 72°C for 30 s; and then a final extension at 72°C for 7 min. Heteroduplexes were generated by thermal cycling under the following conditions: 95°C for 1 min, followed by 45 temperature decrements of 1.5°C/min. PCR products were analyzed with the DHPLC system WAVE (Transgenomic Inc., Omaha, NE, USA). This involved separating PCR products (5 μL) on a heated C18 reverse-phase column using 0.1 M triethylammonium acetate (TEAA) in water and 0.1 M TEAA in 25% acetonitrile at a flow rate of 0.9 mL/min. The temperature for heteroduplex separation of a heterozygous *CYP2A13* fragment was determined with the WAVE software, and the linear acetonitrile gradient was adjusted so that the retention time of the DNA peak was 3–5 min. The resultant chromatograms were compared with those of wild-type DNA, and both DNA strands were sequenced for samples in which variants were detected.

*CYP4B1*1* (wild-type), *CYP4B1*2* (AT881-882del, 993G>A, 1018C>T, and 1123C>T), *CYP4B1*3* (517C>T), *CYP4B1*5* (993G>A), *CYP4B1*6* (517C>T and 1033G>A), and *CYP4B1*7* (AT881-882del, 993G>A, and 1018C>T) were also genotyped by the hybridization probe assay described by Sasaki *et al.*[17] Analysis of the distribution of the five polymorphisms (517C>T, AT881-882del, 993G>A, 1033G>A, and 1123C>T) allowed the characterization of six different *CYP4B1* alleles.

*SULT1A1*1* (wild-type) and *SULT1A1*2* (638G>A) were genotyped by a hybridization probe assay. The PCR mixtures contained 3 mM $MgCl_2$, 0.5 μM each of the PCR primers, 0.4 μM of LC Red 640-labeled hybridization probes, 0.2 μM fluorescein isothiocyanate (FITC)-labeled hybridization probes, 1 μM LightCycler DNA Master Hybridization Mix (Roche Diagnostics Inc., Mannheim, Germany), and approximately 30 ng of genomic DNA in a final volume of 10 μL. The thermal profile consisted of 30 s of initial denaturation at 95°C, followed by 45 cycles at 95°C for 1 s, annealing at 50°C for 5 s, and extension at 72°C for 5 s. The analytical melting program involved melting the PCR products at 95°C for 30 s and at 40°C for 30 s, followed by increasing the temperature to 80°C at a ramp rate of 0.2°C/s, with continuous fluorescence data collection.

GSTM1 and *GSTT1 null* (whole gene deletion) were identified by a multiplex PCR assay described by Abdel-Rahman *et al.*[26] Genomic DNA (10–50 ng) was amplified in a 20-μL reaction mixture containing 0.25 μM of each of the *GSTM1* and *GSTT1* primers. Exon 7 of the *CYP1A1* gene was co-amplified as an internal control. Thermal cycling conditions comprised denaturation at 95°C for 10 min; 30 cycles of denaturation at 95°C for 30 s, annealing at 62°C for 30 s, and extension at 72°C for 30 s; and a final extension at 72°C for 7 min. PCR products from co-amplification of the *GSTM1*, *GSTT1*, and *CYP1A1* genes were analyzed by electrophoresis in 2% agarose gel. The *GSTM1* and *GSTT1* genes were detected by the presence or absence of a 215-bp (corresponding to *GSTM1*) or a 480-bp band (corresponding to *GSTT1*).

Statistical analysis: We evaluated the frequency distribution of patient characteristics, including sex, age, and smoking status, between the lung cancer cases and controls with the chi-squared and unpaired *t*-tests. Hardy-Weinberg equilibrium (HWE) was tested separately for each genotype in the cases and controls. The crude odds ratio (crude OR) and 95% confidence interval (95% CI) were used as estimates of the relative risk. The adjusted OR was calculated using binominal logistic regression to control for sex, age, and smoking status. A two-tailed P value < 0.05 indicated statistical significance. All statistical analyses were performed with Dr. SPSS software (Ver. 11.0.1).

Results

Cases and controls were classified according to sex, age, smoking status, and histological types of lung cancer (**Table 1**). The mean ages at the time of death were 80.3 ± 7.9 years in lung cancer patients and 80.3 ± 7.7 years in the cancer-free controls ($P = 0.991$). There were no statistically significant differences in sex distribution between the two groups (67.2% male cancer patients versus 69.0% male control patients, $P = 0.705$). More smokers were present in the cancer group compared with the control group (70.3% smokers among the cancer patients versus 51.7% smokers among the controls, $P < 0.001$). Of the 192 cancer patients, 41.7% had adenocarcinoma (AC), 24.5% had squamous cell carcinoma (SQCC), 21.4% had small-cell carcinoma (SCC), and 12.4% had other types of lung cancer.

The genotype distributions of *CYP2A6*, *CYP2A13*, *CYP4B1*, *SULT1A1*, *GSTM1*, and *GSTT1* in lung cancer cases and controls are summarized in **Table 2**. The frequency of *CYP2A6*4/*4* in cancer cases was significantly lower than that in the controls (adjusted OR = 0.36, 95% CI = 0.15–0.88, $P = 0.025$). Although the distribution of *CYP2A13*1/*2* (9.4%) and **1/*3* (3.1%) in cancer cases was lower than that in the controls (12.3% and 3.9%, respectively), there was no significant association with lung cancer risk. In addition, the *CYP4B1*, *SULT1A1*, *GSTM1*, and *GSTT1* genotypes were not associated with lung cancer risk.

Table 1. The characteristics of subjects who had lung cancer (cases) and those not having cancer (controls)

Characteristic	Cases (n = 192)	Controls (n = 203)	*P*-value
Gender, n (%)			
Male	129 (67.2)	140 (69.0)	0.705[a]
Female	63 (32.8)	63 (31.0)	
Mean age, n (SD)	80.3 (7.9)	80.3 (7.7)	0.991[b]
Smoking status, n (%)			
Non-smokers	39 (20.3)	78 (38.4)	<0.001[a]
Smokers	135 (70.3)	105 (51.7)	
No information	18 (9.4)	20 (9.9)	
Histological type			
AC	80 (41.7)		
SQCC	47 (24.5)		
SCC	41 (21.4)		
ASQC	4 (2.1)		
LCC	1 (0.5)		
Unknown	7 (3.6)		
AC + SQCC + SCC	1 (0.5)		
SQCC + SCC + ASQC	1 (0.5)		
AC + SQCC	4 (2.1)		
AC + SCC	1 (0.5)		
AC + Unknown	2 (1.0)		
SQCC + SCC	3 (1.6)		

AC, adenocarcinoma; SQCC, squamous cell carcinoma; SCC, small-cell carcinoma; ASQC, adenosquamous cell carcinoma; LCC, large cell carcinoma; SD, Standard deviation.
[a]Chi-squared test, [b]unpaired *t* test.

Table 3 summarizes the relationship between the *CYP2A6* and *CYP2A13* genotypes among lung cancer cases and controls, stratified by smoking status. There was a statistically significant association between smokers carrying *CYP2A6*4/*4* and lung cancer risk (OR = 0.32, 95% CI = 0.10–0.99, $P = 0.049$). ORs were not calculated for non-smokers carrying *CYP2A13*1/*2* and **1/*3*, as the frequency was 0 in cancer cases. There was no statistically significant association between the *CYP4B1*, *SULT1A1*, *GSTM1*, and *GSTT1* genotypes stratified by smoking status and lung cancer risk (data not shown). When stratifying by histological type, no significant association was found for any of the analyzed polymorphisms and lung cancer risk (data not shown).

Discussion

In this study, we observed that polymorphism of the *CYP2A6* gene, but not of the *CYP2A13*, *CYP4B1*, *SULT1A1*, *GSTM1*, or *GSTT1* genes, was associated with decreased risk of lung cancer in the Japanese population studied.

Defective *CYP2A6* alleles have been associated with both increased and decreased risks of lung cancer in different ethnic groups. A Chinese lung cancer study suggested that the presence of the defective allele *CYP2A6*4* increases lung cancer risk.[10] In contrast, a Japanese lung cancer study suggested that the presence of the *CYP2A6*4* allele decreases the risk of lung cancer.[9] The results of our study were consistent with the latter study. CYP2A6 is responsible for the metabolic activation of NNK, one of the components of tobacco smoke. Reducing the production of ultimate carcinogens may lead to decreased DNA damage and reduced cancer development. This hypothesis was supported by a statistically significant association between smokers carrying *CYP2A6*4/*4* and lung cancer risk.

To the best of our knowledge, this is the first case-control study evaluating the relationship between *CYP2A13* genetic polymorphism and lung cancer risk in the Japanese population. CYP2A13 is highly active in the metabolic activation of several carcinogens. Thus, we speculated that reduction in enzymatic activity observed in the *CYP2A13*2* (74G>A and 3375C>T) allelic variant could provide some protection against xenobiotic toxicity. Wang *et al.* reported that Chinese individuals carrying the variant *CYP2A13* allele (3375CT or TT) have a reduced risk of lung adenocarcinoma in relation to light tobacco smoking, but protection against lung squamous cell carcinoma was not observed.[11] Timofeeva *et al.* found no significant association between *CYP2A13* polymorphisms and lung cancer risk in Caucasian patients.[27] We also did not find significant association between the variant *CYP2A13* allele and lung cancer. Interestingly, none of the non-smokers with lung cancer had the CYP2A13*2 or *3 alleles (**Table 3**). In non-smoking individuals with low carcinogenic activity caused by *CYP2A13* polymorphisms, the risk of lung cancer in the population may be much lower than that in smokers with CYP2A13 wild-type genotypes.

The effect of *CYP4B1* polymorphisms on susceptibility of lung cancer has not previously been investigated. Our study is the first to provide evidence that *CYP4B1* polymorphisms may not be associated with lung cancer risk. Our previous study indicated that *CYP4B1* genotypes may affect bladder cancer risk.[17] Thus, the effect of the *CYP4B1* polymorphism may differ among human organs with respect to cancer development.

Since SULT1A1 catalyzes the sulfation of numerous carcinogenic and mutagenic compounds such as heterocyclic and aromatic amines and polycyclic aromatic hydrocarbons, it was suggested that the reduction in enzymatic activity observed in *SULT1A1*2* could affect the risk of lung cancer; however, the association between *SULT1A1*2* and lung cancer risk was not statistically significant in this study. Nevertheless, Liang *et al.* conducted a study on 805 individuals with cancer and 809 control subjects in China, and demonstrated that the lung cancer risk was elevated among individuals with the *SULT1A1*2* allele.[21] The reason for the discrepancy between our results and Liang's is unknown but may be related to differences in ethnicity, sample size, or environmental carcinogen exposure.

Table 2. Genotype and allele frequencies of *CYP2A6*, *CYP2A13*, *CYP4B1*, *SULT1A1*, *GSTM1*, and *GSTT1* polymorphisms among cases and controls and their association with lung cancer

Genotypes	Cases, n (%)	Controls, n (%)	Crude OR[a] (95% CI)	Adjusted OR[b] (95% CI)
CYP2A6				
*non*4/non*4*	122 (63.5)	118 (58.1)	1.00	1.00
*non*4/*4*	63 (32.8)	66 (32.5)	0.92 (0.60–1.42)	0.93 (0.61–1.43)
**4/*4*	7 (3.6)	19 (9.4)	0.36 (0.14–0.88)†	0.36 (0.15–0.88)†
Alleles				
*non*4*	307 (79.9)	302 (74.4)	1.00	
**4*	77 (20.1)	104 (25.6)	0.73 (0.52–1.02)	
CYP2A13				
**1/*1*	163 (84.9)	166 (81.8)	1.00	1.00
**1/*2*	18 (9.4)	25 (12.3)	0.73 (0.39–1.40)	0.75 (0.39–1.44)
**1/*3*	6 (3.1)	8 (3.9)	0.76 (0.26–2.25)	0.77 (0.26–2.27)
Rare genotypes[c]	5 (2.6)	4 (2.0)	—	—
Alleles				
**1*	355 (92.4)	369 (90.9)	1.00	
**2*	18 (4.7)	25 (6.2)	0.75 (0.40–1.40)	
**3*	6 (1.6)	8 (2.0)	0.78 (0.27–2.27)	
CYP4B1				
**1/*1*	52 (27.1)	48 (23.6)	1.00	1.00
**1/*2*	67 (34.9)	61 (30.0)	1.01 (0.60–1.71)	1.00 (0.59–1.70)
**1/*3*	23 (12.0)	32 (15.8)	0.66 (0.34–1.29)	0.65 (0.33–1.27)
**2/*2*	19 (9.9)	20 (9.9)	0.88 (0.42–1.84)	0.88 (0.42–1.84)
**2/*3*	14 (7.3)	16 (7.9)	0.81 (0.36–1.83)	0.80 (0.35–1.81)
**3/*3*	7 (3.6)	7 (3.6)	0.92 (0.30–2.83)	1.00 (0.32–3.14)
Rare genotypes[d]	10 (5.2)	19 (9.4)	—	—
Alleles				
**1*	200 (52.1)	202 (49.8)	1.00	
**2*	122 (31.8)	121 (29.8)	1.02 (0.74–1.40)	
**3*	52 (13.5)	64 (15.8)	0.82 (0.54–1.24)	
SULT1A1				
**1/*1*	120 (62.5)	132 (65.0)	1.00	1.00
**1/*2*	70 (36.5)	68 (33.5)	1.13 (0.75–1.72)	1.12 (0.74–1.70)
**2/*2*	2 (1.0)	3 (1.5)	0.73 (0.12–4.46)	0.76 (0.12–4.71)
Alleles				
**1*	310 (80.7)	332 (81.8)	1.00	
**2*	74 (19.3)	74 (18.2)	1.07 (0.75–1.53)	
GSTM1				
Present	106 (55.2)	101 (49.8)	1.00	1.00
Null	86 (44.8)	102 (50.2)	0.80 (0.54–1.19)	0.80 (0.54–1.20)
GSTT1				
Present	95 (49.5)	99 (48.8)	1.00	1.00
Null	97 (50.5)	104 (51.2)	0.97 (0.66–1.44)	0.97 (0.65–1.44)

OR, odds ratio; CI, confidence interval.
†$P < 0.05$ (vs. *CYP2A6 non*4/non*4*).
[a]Chi-squared test. [b]Binominal logistic regression analysis adjusted by sex, age, and smoking status.
[c]Rare genotypes included: *CYP2A13*1/*4*, *CYP2A13*1/*5*, *CYP2A13*1/*7*, and *CYP2A13*1*10*.[25]
[d]Rare genotypes included: *CYP4B1*1/*5*, *CYP4B1*1/*6*, *CYP4B1*1/*7*, *CYP4B1*2/*5*, *CYP4B1*2/*6*, *CYP4B1*2/*7*, and *CYP4B1*3/*7*.

Table 3. Effect of *CYP2A6* and *CYP2A13* genotypes by smoking status on lung cancer risk

Genotypes	Smokers			Non-smokers		
	Cases/controls	Adjusted OR[a] (95% CI)	*P*-value	Cases/controls	Adjusted OR[a] (95% CI)	*P*-value
CYP2A6						
*non*4/non*4*	87/52	1.00		22/53	1.00	
*non*4/*4*	43/43	0.61 (0.35–1.05)	0.074	15/18	2.35 (0.96–5.72)	0.060
**4/*4*	5/10	0.32 (0.10–0.99)	0.049	2/7	0.74 (0.14–4.01)	0.724
CYP2A13						
**1/*1*	109/80	1.00		38/69	1.00	
**1/*2*	17/19	0.68 (0.33–1.40)	0.293	0/5	—	—
**1/*3*	5/3	1.51 (0.35–6.58)	0.585	0/3	—	—

OR, odds ratio; CI, confidence interval.
[a]Binominal logistic regression analysis adjusted by sex and age.

In the present study, there was no statistically significant association between either the *GSTM1* or *GSTT1* genotype and lung cancer risk in the Japanese subjects studied. To-Figueras *et al.* reported that 14.4% of their cancer patients possessed homozygous deletion of both *GSTT1* and *GSTM1* (12.5% among healthy smokers),[28] suggesting no potentiation between null genotypes for lung cancer risk, which is in agreement with our results. In contrast, Pinarbasi *et al.*[23] and Kihara *et al.*[22] reported that *GSTM1* null genotypes were associated with lung cancer risk in a Turkish population and in male Japanese smokers, respectively. These conflicting results, including ours, may be caused by some confounding factors such as ethnicity, selection of control group, characterization of cases, sample size, gene-gene and gene-environment interactions, and second-hand smoke conditions.

In conclusion, these results indicate that the *CYP2A6*4/*4* genotypes, but not the *CYP2A13*, *CYP4B1*, *SULT1A1*, *GSTM1*, and *GSTT1* gene polymorphisms, were associated with decreased risk of lung cancer in the Japanese population studied. However, there is an element of chance in the results in the present study because the sample size was relatively small. Therefore, further studies with larger sample sizes will be required to confirm the present findings.

Acknowledgment: We thank the Biomedical Research Core of Tohoku University Graduate School of Medicine for technical support.

References

1) Greenlee, R. T., Murray, T., Bolden, S. and Wingo, P. A.: Cancer statistics, 2000. *CA Cancer J. Clin.*, **50**: 7–33 (2000).
2) Petrauskaitė, R., Pershagen, G. and Gurevicius, R.: Lung cancer near an industrial site in Lithuania with major emissions of airway irritants. *Int. J. Cancer*, **99**: 106–111 (2002).
3) Stellman, S. D., Takezaki, T., Wang, L., Chen, Y., Citron, M. L., Djordjevic, M. V., Harlap, S., Muscat, J. E., Neugut, A. I., Wynder, E. L., Ogawa, H., Tajima, K. and Aoki, K.: Smoking and lung cancer risk in American and Japanese men: an international case-control study. *Cancer Epidemiol. Biomarkers Prev.*, **10**: 1193–1199 (2001).
4) Bao, Z., He, X. Y., Ding, X., Prabhu, S. and Hong, J. Y.: Metabolism of nicotine and cotinine by human cytochrome P450 2A13. *Drug Metab. Dispos.*, **33**: 258–261 (2005).
5) Su, T., Bao, Z., Zhang, Q. Y., Smith, T. J., Hong, J. Y. and Ding, X.: Human cytochrome P450 CYP2A13: predominant expression in the respiratory tract and its high efficiency metabolic activation of a tobacco-specific carcinogen, 4-(methylnitrosamino)-1-(3-pyridyl)-1-butanone. *Cancer Res.*, **60**: 5074–5079 (2000).
6) Koskela, S., Hakkola, J., Hukkanen, J., Pelkonen, O., Sorri, M., Saranen, A., Anttila, S., Fernandez-Salguero, P., Gonzalez, F. and Raunio, H.: Expression of CYP2A genes in human liver and extrahepatic tissues. *Biochem. Pharmacol.*, **57**: 1407–1413 (1999).
7) Nunoya, K., Yokoi, T., Kimura, K., Inoue, K., Kodama, T., Funayama, M., Nagashima, K., Funae, Y., Green, C., Kinoshita, M. and Kamataki, T.: A new deleted allele in the human cytochrome P450 2A6 (CYP2A6) gene found in individuals showing poor metabolic capacity to coumarin and (+)-cis-3,5-dimethyl-2-(3-pyridyl)thiazolidin-4-one hydrochloride (SM-12502). *Pharmacogenetics*, **8**: 239–250 (1998).
8) Ariyoshi, N., Miyamoto, M., Umetsu, Y., Kunitoh, H., Dosaka-Akita, H., Sawamura, Y., Yokota, J., Nemoto, N., Sato, K. and Kamataki, T.: Genetic polymorphism of CYP2A6 gene and tobacco-induced lung cancer risk in male smokers. *Cancer Epidemiol. Biomarkers Prev.*, **11**: 890–894 (2002).
9) Fujieda, M., Yamazaki, H., Saito, T., Kiyotani, K., Gyamfi, M. A., Sakurai, M., Dosaka-Akita, H., Sawamura, Y., Yokota, J., Kunitoh, H. and Kamataki, T.: Evaluation of CYP2A6 genetic polymorphisms as determinants of smoking behavior and tobacco-related lung cancer risk in male Japanese smokers. *Carcinogenesis*, **25**: 2451–2458 (2004).
10) Tan, W., Chen, G. F., Xing, D. Y., Song, C. Y., Kadlubar, F. F. and Lin, D. X.: Frequency of CYP2A6 gene deletion and its relation to risk of lung and esophageal cancer in the Chinese population. *Int. J. Cancer*, **95**: 96–101 (2001).
11) Wang, H., Tan, W., Hao, B., Miao, X., Zhou, G., He, F. and Lin, D.: Substantial reduction in risk of lung adenocarcinoma associated with genetic polymorphism in CYP2A13, the most active cytochrome P450 for the metabolic activation of tobacco-specific carcinogen NNK. *Cancer Res.*, **63**: 8057–8061 (2003).
12) Choudhary, D., Jansson, I., Stoilov, I., Sarfarazi, M. and Schenkman, J. B.: Expression patterns of mouse and human CYP orthologs (families 1-4) during development and in different adult tissues. *Arch. Biochem. Biophys.*, **436**: 50–61 (2005).
13) Imaoka, S., Yoneda, Y., Sugimoto, T., Hiroi, T., Yamamoto, K., Nakatani, T. and Funae, Y.: CYP4B1 is a possible risk factor for

bladder cancer in humans. *Biochem. Biophys. Res. Commun.*, **277**: 776–780 (2000).
14) Imaoka, S., Yoneda, Y., Matsuda, T., Degawa, M., Fukushima, S. and Funae, Y.: Mutagenic activation of urinary bladder carcinogens by CYP4B1 and the presence of CYP4B1 in bladder mucosa. *Biochem. Pharmacol.*, **54**: 677–683 (1997).
15) Vanderslice, R. R., Boyd, J. A., Eling, T. E. and Philpot, R. M.: The cytochrome P-450 monooxygenase system of rabbit bladder mucosa: enzyme components and isozyme 5-dependent metabolism of 2-aminofluorene. *Cancer Res.*, **45**: 5851–5858 (1985).
16) Hiratsuka, M., Nozawa, H., Konno, Y., Saito, T., Konno, S. and Mizugaki, M.: Human CYP4B1 gene in the Japanese population analyzed by denaturing HPLC. *Drug Metab. Pharmacokinet.*, **19**: 114–119 (2004).
17) Sasaki, T., Horikawa, M., Orikasa, K., Sato, M., Arai, Y., Mitachi, Y., Mizugaki, M., Ishikawa, M. and Hiratsuka, M.: Possible relationship between the risk of Japanese bladder cancer cases and the CYP4B1 genotype. *Jpn. J. Clin. Oncol.*, **38**: 634–640 (2008).
18) Falany, C. N.: Enzymology of human cytosolic sulfotransferases. *FASEB J.*, **11**: 206–216 (1997).
19) Richard, K., Hume, R., Kaptein, E., Stanley, E. L., Visser, T. J. and Coughtrie, M. W.: Sulfation of thyroid hormone and dopamine during human development: ontogeny of phenol sulfotransferases and arylsulfatase in liver, lung, and brain. *J. Clin. Endocrinol. Metab.*, **86**: 2734–2742 (2001).
20) Arslan, S., Silig, Y. and Pinarbasi, H.: An investigation of the relationship between SULT1A1 Arg(213)His polymorphism and lung cancer susceptibility in a Turkish population. *Cell Biochem. Funct.*, **27**: 211–215 (2009).
21) Liang, G., Miao, X., Zhou, Y., Tan, W. and Lin, D.: A functional polymorphism in the SULT1A1 gene (G638A) is associated with risk of lung cancer in relation to tobacco smoking. *Carcinogenesis*, **25**: 773–778 (2004).
22) Kihara, M. and Noda, K.: Risk of smoking for squamous and small cell carcinomas of the lung modulated by combinations of CYP1A1 and GSTM1 gene polymorphisms in a Japanese population. *Carcinogenesis*, **16**: 2331–2336 (1995).
23) Pinarbasi, H., Silig, Y., Cetinkaya, O., Seyfikli, Z. and Pinarbasi, E.: Strong association between the GSTM1-null genotype and lung cancer in a Turkish population. *Cancer Genet. Cytogenet.*, **146**: 125–129 (2003).
24) Oscarson, M., McLellan, R. A., Gullsten, H., Yue, Q. Y., Lang, M. A., Bernal, M. L., Sinues, B., Hirvonen, A., Raunio, H., Pelkonen, O. and Ingelman-Sundberg, M.: Characterisation and PCR-based detection of a CYP2A6 gene deletion found at a high frequency in a Chinese population. *FEBS Lett.*, **448**: 105–110 (1999).
25) Tamaki, Y., Honda, M., Muroi, Y., Arai, T., Sugimura, H., Matsubara, Y., Kanno, S., Ishikawa, M., Hirasawa, N. and Hiratsuka, M.: Novel single nucleotide polymorphism of the CYP2A13 gene in Japanese individuals. *Drug Metab. Pharmacokinet.*, in press (2011).
26) Abdel-Rahman, S. Z., el-Zein, R. A., Anwar, W. A. and Au, W. W.: A multiplex PCR procedure for polymorphic analysis of GSTM1 and GSTT1 genes in population studies. *Cancer Lett.*, **107**: 229–233 (1996).
27) Timofeeva, M. N., Kropp, S., Sauter, W., Beckmann, L., Rosenberger, A., Illig, T., Jager, B., Mittelstrass, K., Dienemann, H., Bartsch, H., Bickeboller, H., Chang-Claude, J. C., Risch, A. and Wichmann, H. E.: CYP450 polymorphisms as risk factors for early-onset lung cancer: gender-specific differences. *Carcinogenesis*, **30**: 1161–1169 (2009).
28) To-Figueras, J., Gene, M., Gomez-Catalan, J., Galan, M. C., Fuentes, M., Ramon, J. M., Rodamilans, M., Huguet, E. and Corbella, J.: Glutathione S-transferase M1 (GSTM1) and T1 (GSTT1) polymorphisms and lung cancer risk among Northwestern Mediterraneans. *Carcinogenesis*, **18**: 1529–1533 (1997).

0090-9556/11/3910-1860–1865$25.00
DRUG METABOLISM AND DISPOSITION
Vol. 39, No. 10
40352/3717294
Printed in U.S.A.

DMD 39:1860–1865, 2011

Functional Characterization of CYP2B6 Allelic Variants in Demethylation of Antimalarial Artemether

Masashi Honda, Yuka Muroi, Yuichiro Tamaki, Daisuke Saigusa, Naoto Suzuki, Yoshihisa Tomioka, Yoichi Matsubara, Akifumi Oda, Noriyasu Hirasawa, and Masahiro Hiratsuka

Laboratory of Pharmacotherapy of Life-Style Related Diseases (M.H., Y.Mu., Y.Ta., N.H., M.H.) and Laboratory of Oncology, Pharmacy Practice and Sciences, Graduate School of Pharmaceutical Sciences, Tohoku University, Sendai, Japan (D.S., N.S., Y.To.); Department of Medical Genetics, Tohoku University School of Medicine, Sendai, Japan (Y.Ma.); and Faculty of Pharmaceutical Sciences, Tohoku Pharmaceutical University, Sendai, Japan (A.O.)

Received May 5, 2011; accepted July 11, 2011

ABSTRACT:

Artemether (AM) is one of the most effective antimalarial drugs. The elimination half-life of AM is very short, and it shows large interindividual variability in pharmacokinetic parameters. The aim of this study was to identify cytochrome P450 (P450) isozymes responsible for the demethylation of AM and to evaluate functional differences between 26 CYP2B6 allelic variants in vitro. Of 14 recombinant P450s examined in this study, CYP2B6 and CYP3A4 were primarily responsible for production of the desmethyl metabolite dihydroartemisinin. The intrinsic clearance (V_{max}/K_m) of CYP2B6 was 6-fold higher than that of CYP3A4. AM demethylation activity was correlated with CYP2B6 protein levels ($P = 0.004$); however, it was not correlated with CYP3A4 protein levels ($P = 0.27$) in human liver microsomes. Wild-type CYP2B6.1 and 25 CYP2B6 allelic variants (CYP2B6.2-CYP2B6.21 and CYP2B6.23-CYP2B6.27) were heterologously expressed in COS-7 cells. In vitro analysis revealed no enzymatic activity in 5 variants (CYP2B6.8, CYP2B6.12, CYP2B6.18, CYP2B6.21, and CYP2B6.24), lower activity in 7 variants (CYP2B6.10, CYP2B6.11, CYP2B6.14, CYP2B6.15, CYP2B6.16, CYP2B6.20, and CYP2B6.27), and higher activity in 4 variants (CYP2B6.2, CYP2B6.4, CYP2B6.6, and CYP2B6.19), compared with that of wild-type CYP2B6.1. In kinetic analysis, 3 variants (CYP2B6.2, CYP2B6.4, and CYP2B6.6) exhibited significantly higher V_{max}, and 3 variants (CYP2B6.14, CYP2B6.20 and CYP2B6.27) exhibited significantly lower V_{max} compared with that of CYP2B6.1. This functional analysis of CYP2B6 variants could provide useful information for individualization of antimalarial drug therapy.

Introduction

Malaria is a very serious problem in many countries, and there are more than 200 million cases that result in approximately 1 million deaths worldwide each year (World Health Organization, World Malaria Report 2009, http://www.who.int/malaria/world_malaria_report_2009/en/index.html). The management of malaria has traditionally relied on monotherapy with quinolines such as quinine, mefloquine, and chloroquine. However, the widespread and excessive use of these agents has resulted in drug resistance (Wernsdorfer, 1991; Price and Nosten, 2001; Le Bras and Durand, 2003). In several studies, artemisinins, unique sesquiterpene lactone endoperoxides, have been used in areas with multidrug-resistant *Plasmodium falciparum* malaria (Woodrow et al., 2005; Gautam et al., 2009; World Health Organization, 2010).

This work was supported by the Japan Society for the Promotion of Science [KAKENHI 20590154] and in part by the Smoking Research Foundation.

Article, publication date, and citation information can be found at http://dmd.aspetjournals.org.

doi:10.1124/dmd.111.040352.

Artemisinin is a natural antimalarial agent derived from the Chinese medicinal plant *Artemisia annua* (Klayman, 1985). The artemisinin derivative artemether (AM) is the most effective antimalarial drug. AM has a fast onset of action, therapeutic efficacy against multidrug-resistant malaria, and few side effects, although neurotoxicity has been observed in experimental mammals (Hien and White, 1993; Brewer et al., 1994). AM is mainly converted to dihydroartemisinin (DHA) (Fig. 1), a desmethyl metabolite that contributes to the majority of the antimalarial activity. The conversion of AM to DHA is catalyzed by cytochrome P450 (P450) (van Agtmael et al., 1999b,c; Navaratnam et al., 2000). However, the elimination half-life of AM is very short, and it shows large interindividual variability in pharmacokinetic parameters (Na Bangchang et al., 1994; Mordi et al., 1997; van Agtmael et al., 1999a; Lefèvre et al., 2002; Ali et al., 2010; Mwesigwa et al., 2010).

The P450 isozymes CYP2B6 and CYP3A4 are thought to catalyze AM demethylation (Navaratnam et al., 2000). In contrast, it has been reported that CYP2D6 and CYP2C19 make no major contribution to this reaction (van Agtmael et al., 1998), and the role of other P450s remains unclear. CYP2B6 plays a major role in the biotransformation of several therapeutically important drugs, including cyclophosph-

ABBREVIATIONS: AM, artemether; DHA, dihydroartemisinin; P450, cytochrome P450; ART, artemisinin; LC, liquid chromatography; MS/MS, tandem mass spectrometry.

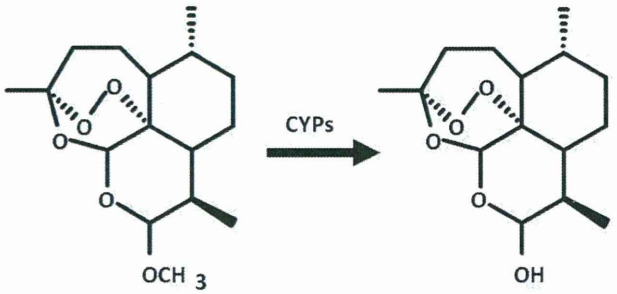

FIG. 1. Metabolic pathway of artemether to dihydroartemisinin by P450 enzymes.

amide, bupropion, selegiline, efavirenz, nevirapine, and methadone (Roy et al., 1999; Hesse et al., 2000; Hidestrand et al., 2001; Salonen et al., 2003). Many genetic polymorphisms in the *CYP2B6* gene have been reported, and these are thought to be responsible for interindividual and interethnic differences in responses to CYP2B6 substrate drugs [Zanger et al., 2007; Human Cytochrome P450 (CYP) Allele Nomenclature Committee, 2008; Mo et al., 2009]. In the case of chemotherapy using cyclophosphamide, the increasing enzymatic activity of CYP2B6 variants can be associated with the increased blood concentration of the active metabolite of the drug, resulting in a heightened risk of side effects (Xie et al., 2003, 2006; Nakajima et al., 2007).

Several functional analyses of CYP2B6 variant proteins, using an in vitro expression system, have been reported. Watanabe et al. (2010) characterized the functional relevance of many CYP2B6 variants, including CYP2B6.1 to CYP2B6.28, using 7-ethoxy-4-trifluoromethylcoumarin and selegiline as substrates, and reported that CYP2B6.8, CYP2B6.11, CYP2B6.12, CYP2B6.13, CYP2B6.15, CYP2B6.18, CYP2B6.21, CYP2B6.24, and CYP2B6.28 were inactive with regard to these compounds. These results were consistent with those of a number of in vitro studies using bupropion as a substrate. In contrast, CYP2B6.16, CYP2B6.19, and CYP2B6.27 exhibited activity toward 7-ethoxy-4-trifluoromethylcoumarin and inability to detect selegiline metabolism. Several researchers have reported that these CYP2B6 variants exhibited decreased protein expression/activity when bupropion was used as the CYP2B6 substrate (Lang et al., 2004; Klein et al., 2005; Wang et al., 2006; Rotger et al., 2007). These results suggest that some allelic variants of CYP2B6 are associated with a substrate-dependent decrease in the catalytic properties of the enzyme. To date, there have been no reports of functional characterization of CYP2B6 variants in relation to AM demethylation activity.

In this study, we performed an in vitro analysis of 14 P450s (CYP1A1, CYP1A2, CYP1B1, CYP2A6, CYP2B6, CYP2C8, CYP2C9, CYP2C19, CYP2D6, CYP2E1, CYP2J2, CYP3A4, CYP3A5, and CYP4A11) to identify isoforms responsible for AM demethylation and evaluated functional differences among 26 CYP2B6 allelic variants (Fig. 2).

Materials and Methods

Chemicals. AM, DHA, and artemisinin (ART) were purchased from Tokyo Chemical Industry Corporation (Tokyo, Japan). Recombinant CYP1A1, CYP2A6, CYP2B6, CYP2C8, CYP2D6, CYP2J2, and CYP4A11 Supersomes were purchased from BD Biosciences (Woburn, MA). CYP1A2, CYP2C9, CYP2E1, CYP3A4, and CYP3A5 Baculosomes were purchased from Invitrogen (Carlsbad, CA). NADPH was obtained from Oriental Yeast (Tokyo, Japan). Protease Inhibitor Cocktail Set III was purchased from Merck Chemicals (Darmstadt, Germany). Methanol (CH_3OH) and acetonitrile (CH_3CN) of LC-mass spectrometry grade were obtained from Kanto Chemical (Tokyo, Japan). Ammonium formate ($HCOONH_4$) and formic acid (HCOOH) of LC-mass spectrometry grade were obtained from Wako Pure Chemical Industries (Tokyo, Japan).

DHA stock solution (5 mM) was prepared in CH_3CN/H_2O [50:50 (v/v)], and working solutions (1.0, 2.0, 5.0, 10, 25, 50, 100, and 200 μM) were prepared from the stock solution. These solutions were further diluted in 50 mM potassium phosphate buffer, pH 7.4, and the final calibration curves were obtained with 0.1, 0.2, 0.5, 1.0, 2.5, 5.0, 10, and 20 μM solutions. Working solutions (100 μl) were prepared in 1.5-ml plastic tubes, and 100 μl of CH_3OH, 5 μl of internal standard (ART at 100 μM), and 100 μl of H_2O were

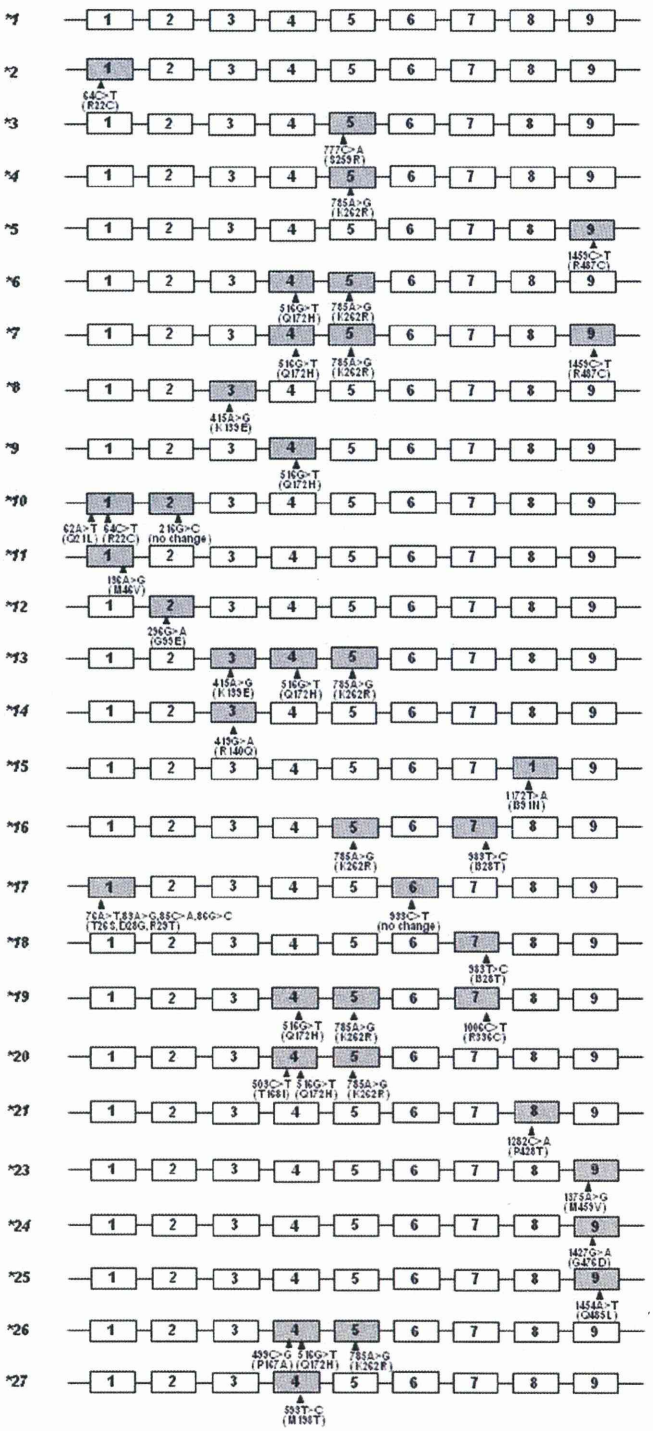

FIG. 2. Structures of CYP2B6 alleles characterized in this study. The nine exons are indicated by numbered boxes. Some promoter and intronic polymorphisms are not shown.

added. The resulting mixture was vortexed. After centrifugation at 12,000*g* for 10 min, 80 μl of the supernatant was transferred to a new plastic tube and passed through a filter (pore size: 0.2 μm; YMC Co., Ltd., Kyoto, Japan). Subsequently, 10 μl of the filtered solution was injected into the liquid chromatography-tandem mass spectrometry (LC-MS/MS) system for analysis. All peaks were integrated automatically by Xcalibur software (Thermo Fisher Scientific, Waltham, MA). Levels of DHA were calculated from the calibration curves by the ratios of their peak areas to that of ART. An eight-point calibration curve was plotted for DHA concentration (0.1, 0.2, 0.5, 1.0, 2.5, 5.0, 10, and 20 μM).

Sample Preparation for Analysis of Specific Activity. AM demethylation activity was determined by measurement of the formation of DHA, according to the method of Asimus and Ashton (2009), with minor modifications. AM stock solution (50 mM) was prepared in CH_3CN/H_2O [50:50 (v/v)], and a working solution (500 μM) was prepared by dilution of the stock solution in potassium phosphate buffer, pH 7.4. The incubation mixture contained AM as a substrate (1 and 50 μM), recombinant P450 enzymes (CYP1A1, CYP1A2, CYP1B1, CYP2A6, CYP2B6, CYP2C8, CYP2C9, CYP2C19, CYP2D6, CYP2E1, CYP2J2, CYP3A4, CYP3A5, and CYP4A11; 0.5 pmol) or human liver microsomes (50 μg), 0.5 mM NADPH, 5 mM $MgCl_2$, and 50 mM potassium phosphate buffer to a final volume of 90 μl. After preincubation (3 min at 37°C), the reaction was started by addition of NADPH. Reactions were performed for 30 min and terminated by the addition of 100 μl of methanol. Then, 5 μl of internal standard (ART at 100 μM) and 100 μl of H_2O were added. The resulting mixture was vortexed. After centrifugation at 12,000*g* for 10 min, 80 μl of the supernatant was transferred to a new plastic tube and passed through a filter (pore size: 0.2 μm; YMC). Then, 10 μl of the filtered solution was injected into the LC-MS/MS system for analysis. All peaks were integrated automatically by Xcalibur software. Levels of DHA were calculated from the calibration curves by using the ratios of their peak areas to that of ART. Formation of DHA was in the linear range between 10 and 60 min and 30 and 50 μg of microsomal protein.

Sample Preparation for Analysis of Kinetic Parameters of CYP2B6 and CYP3A4. AM stock solution (50 mM) was prepared in CH_3CN/H_2O [50:50 (v/v)], and working solutions (0.25, 0.50, 1.25, 2.5, 5.0, 12.5, and 25 mM) were prepared by dilution of the stock solution. These solutions were diluted with 50 mM potassium phosphate buffer, pH 7.4, and the final calibration curves were obtained with 0.5, 1.0, 2.5, 5.0, 10, 25, 50, and 100 μM. CYP2B6 and CYP3A4 activity was evaluated using the concentration ranges 0.5 to 50 and 2.5 to 100 μM, respectively. Samples were prepared as described above.

Determination of DHA and ART Using Online Column-Switching LC-MS/MS. Levels of DHA were determined by the LC-MS/MS method described by Huang et al. (2009), with minor modifications. A Nanospace SI-2 LC system, comprising an LC pump, autosampler, column oven maintained at 40°C, and on-line degasser (Shiseido, Tokyo, Japan), was used. The on-line column-switching valve system consisted of an automated switching valve (six-port valve) connected to pump A and pump B. Pump A was connected via the switching valve to the trap column, a CAPCELL PAK C18 SG II (10 × 2 mm i.d., 3-μm particle size) (Shiseido, Tokyo, Japan), and pump B was connected via the switching valve to the analytical column, a Sunfire C18 (150 mm × 2.1 mm i.d., 3.5-μm particle size) (Waters, Milford, MA). The outlet of the analytical column was connected to the mass spectrometer via a divert valve.

Sample loading. A 10-μl aliquot of sample was injected onto the trap column using pump B with the switching valve in position 1. Impurities on the trap column were eluted to waste using 0.1% HCOOH-H_2O/CH_3CN [5:95 (v/v)] at a flow rate of 200 μl/min for 4 min. Concurrently, initial flow was maintained by pump A at 200 μl/min with 10 mM $HCOONH_4$-H_2O (adjusted to pH 4.1 using HCOOH)-0.1% HCOOH-CH_3CN [20:80 (v/v)] via the analytical column.

Sample elution. At 4 min, the switching valve was switched to position 2 to allow the purified DHA and ART to be eluted from the trap column onto the analytical column and subsequently into the mass spectrometer. Isocratic flow was maintained by pump B at a rate of 200 μl/min for 11 min. Concurrently, the flow from pump A was passed through the trap column and diverted directly to waste. At 11 min, the switching valve was switched back to position 1, and the configuration of the online column switching system reverted back to that in the initial conditions (described for the sample loading above). A divert valve was used to divert the LC effluent to waste during the first 4.5 min and last 0.5 min of the chromatographic run. The total run time was 11 min.

Quantification analyses by MS were performed in the selected reaction monitoring mode because of the high selectivity and sensitivity of selected reaction monitoring data acquisition, in which the transitions of the precursor ion into the product ion were monitored: *m/z* 302 → 145 and 302 → 267 for DHA and *m/z* 300 → 151 and 300 → 209 for ART. The optimized parameters for MS are as follows: positive heated electrospray ionization voltage, 3 kV; heated capillary temperature, 300°C; sheath gas pressure, 50 psi; auxiliary gas setting, 20 psi; and heated vaporizer temperature, 300°C. Both the sheath and auxiliary gases were nitrogen. The collision gas was argon at a pressure of 1.5 mTorr. The LC-MS/MS system was controlled by Xcalibur software, and data were also collected with this software. The retention times of DHA and ART were 7.0 and 7.5 min, respectively.

Liver Specimens. Human liver specimens were obtained from the Human and Animal Bridging Research Organization (HAB) in Chiba, Japan, using frozen human livers (most of the donors were white). Microsomes were prepared from these specimens using differential centrifugation. Research protocols were approved by the ethics committees of the Graduate School of Pharmaceutical Sciences, Tohoku University (Sendai, Japan).

Expression of CYP2B6 Variant Proteins in COS-7 Cells. CYP2B6 variant proteins were expressed in COS-7 cells as described by Watanabe et al. (2010).

Determination of Protein Expression Levels by Immunoblotting. Western blotting was performed according to standard procedures, with 10% SDS-polyacrylamide gel electrophoresis, and 30-μg microsomal fractions were loaded into each lane. Recombinant CYP2B6 Supersomes reagent (BD Gentest) was coanalyzed as the standard on each gel and used to quantify the CYP2B6 protein. The CYP2B6 protein was detected using the antihuman CYP2B6 antibody (BD Gentest) and horseradish peroxidase-conjugated goat anti-rabbit IgG (Dako Denmark A/S, Glostrup, Denmark). CYP3A4 Baculosomes reagent (Invitrogen) was coanalyzed as the standard on each gel and used to quantify the CYP3A4 protein. The CYP3A4 protein was detected using the antihuman CYP3A4 antibody (Nosan, Yokohama, Japan) and horseradish peroxidase-conjugated goat anti-rabbit IgG (Dako Denmark A/S). Immuno-

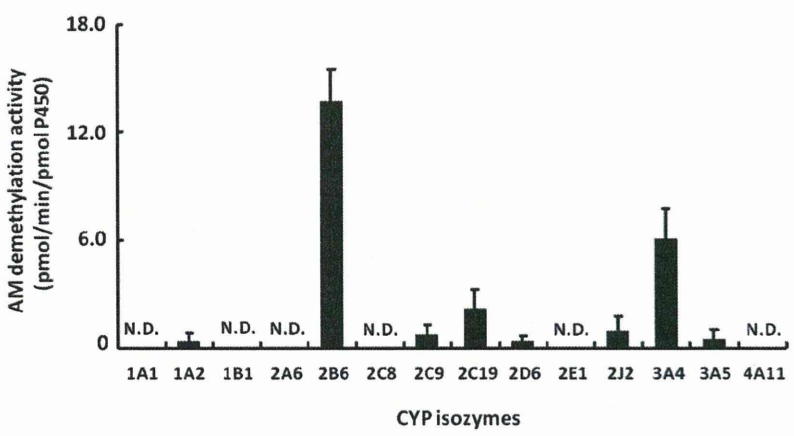

FIG. 3. AM demethylation activity of 14 P450 isozymes. The concentration of AM was 50 μM. Each number corresponds to a P450 subtype. Results are presented as the mean ± S.D. in triplicate. N.D., not detectable (activities were lower than 0.22 pmol · min^{-1} · pmol $P450^{-1}$).

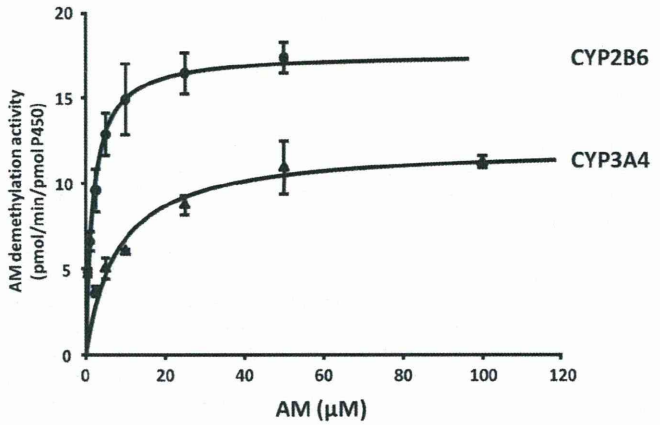

FIG. 4. The Michaelis-Menten curves for the demethylation of AM with recombinant CYP2B6 and CYP3A4.

blots were developed using the SuperSignal West Dura Extended Duration Substrate (Thermo Fisher Scientific). Chemiluminescence was quantified using a lumino-imaging analyzer (LAS-1000; Fujifilm, Tokyo, Japan) and ImageJ software (National Institutes of Health, Bethesda, MD).

Sample Preparation for Analysis of Kinetic Parameters of CYP2B6 Variants. Microsomal fractions (50 μg) obtained from COS-7 cells were used for evaluation of the activity of CYP2B6 variants. Samples were prepared as described above.

Statistical Analysis. Apparent K_m and V_{max} parameters were determined using nonlinear regression analysis. All data are the mean ± S.D. in triplicate. Statistical analyses of enzymatic activities and kinetic parameters were performed by analysis of variance using the Dunnett method. $P \leq 0.05$ was considered significant.

Results

AM Demethylation by Recombinant Human P450s. The activities of AM demethylation were measured in 14 recombinant human P450 enzymes (CYP1A1, CYP1A2, CYP1B1, CYP2A6, CYP2B6, CYP2C8, CYP2C9, CYP2C19, CYP2D6, CYP2E1, CYP2J2, CYP3A4, CYP3A5, and CYP4A11) at 1 and 50 μM substrate concentrations. The lower concentration used was intended to approximate the plasma AM concentrations reported to be clinically relevant (0.3–1 μM) (Ali et al., 2010). At 1 μM AM, AM demethylation activities of recombinant CYP2B6 and CYP3A4 were 6.61 and 2.50 pmol · min^{-1} · pmol P450^{-1}, respectively. Under the lower substrate conditions used in this study, DHA was not formed by the other P450 isoforms with the exception of CYP2B6 and CYP3A4. At a higher concentration (50 μM), AM was principally metabolized by CYP2B6, followed by CYP3A4. A low rate of demethylation was observed for CYP1A2, CYP2C9, CYP2C19, CYP2D6, CYP2J2, and CYP3A5; CYP1A1, CYP1B1, CYP2A6, CYP2C8, CYP2E1, and CYP4A11 were inactive (Fig. 3).

Kinetics of AM Demethylation by CYP2B6 and CYP3A4. The kinetics of AM demethylation were investigated for each of recombinant enzymes CYP2B6 and CYP3A4 by Michaelis-Menten plots (Fig. 4). Apparent K_m, V_{max}, and V_{max}/K_m values for CYP2B6 were estimated to be 1.95 μM, 17.9 pmol · min^{-1} · pmol P450^{-1}, and 9.19 μl · min^{-1} · pmol P450^{-1}, respectively; those for CYP3A4 were 8.24 μM, 12.3 pmol · min^{-1} · pmol P450^{-1}, and 1.49 μl · min^{-1} · pmol P450^{-1}, respectively, demonstrating a higher K_m and lower V_{max}, which resulted in an approximately one-sixth V_{max}/K_m value for CYP3A4 relative to that for CYP2B6.

Comparison of AM Demethylation Activities (at 50 μM AM) to Immunoquantified CYP2B6 and CYP3A4 Protein Levels in 13 Human Liver Microsomes. As shown in Fig. 5, AM demethylation activity in 13 human liver microsomes was correlated with immunoquantified CYP2B6 content ($r^2 = 0.548$, $P = 0.004$) but not with immunoquantified CYP3A4 content ($r^2 = 0.109$, $P = 0.272$).

Enzymatic Properties for AM Demethylation by Wild-Type and 25 Variant CYP2B6s. The demethylation activities of wild-type and 25 variant microsomal CYP2B6 proteins were determined using AM (50 μM) as a substrate (Fig. 6). For CYP2B6.8, CYP2B6.12, CYP2B6.18, CYP2B6.21, and CYP2B6.24, no AM demethylation activity was detected. The enzymatic activity of CYP2B6.3 could not be calculated because its expression level could not be determined by immunoblotting. CYP2B6.10, CYP2B6.11, CYP2B6.14, CYP2B6.15, CYP2B6.16, CYP2B6.20, and CYP2B6.27 exhibited significantly decreased activities compared with that of wild-type CYP2B6.

The Michaelis-Menten kinetics for AM demethylation were determined for CYP2B6.1, CYP2B6.2, CYP2B6.4, CYP2B6.5, CYP2B6.6, CYP2B6.7, CYP2B6.9, CYP2B6.10, CYP2B6.13, CYP2B6.14, CYP2B6.17, CYP2B6.19, CYP2B6.20, CYP2B6.23, CYP2B6.25, CYP2B6.26, and CYP2B6.27. The kinetic parameters are summarized in Table 1. The estimated kinetic parameters, apparent K_m, V_{max}, and V_{max}/apparent K_m for AM demethylation by CYP2B6.1 were 3.10 μM, 36.0 pmol · min^{-1} · pmol CYP2B6^{-1}, and 12.4 μl · min^{-1} · pmol CYP2B6^{-1}, respectively. The V_{max} values for CYP2B6.14, CYP2B6.20, and CYP2B6.27 were significantly decreased, whereas those for CYP2B6.2, CYP2B6.4, and CYP2B6.6 were significantly increased, relative to that for the wild-type enzyme.

Discussion

In this study, we have determined the human P450 enzymes responsible for AM demethylation. Among 14 human P450s, CYP2B6

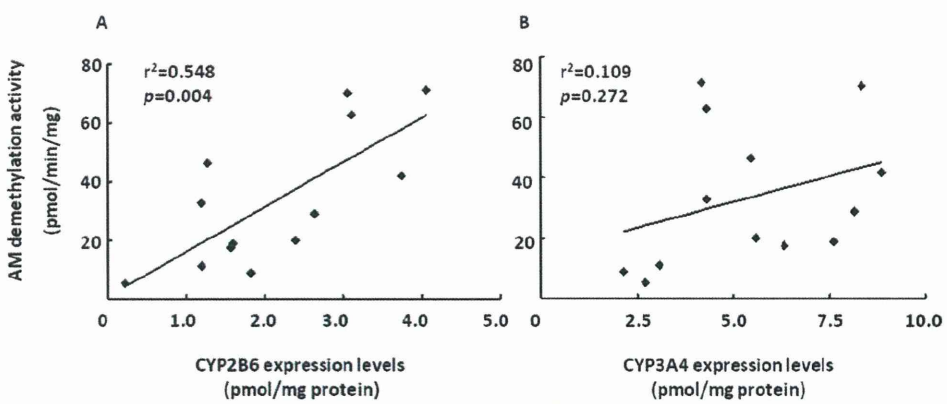

FIG. 5. Comparison of AM demethylation activities (at 50 μM AM) to immunoquantified CYP2B6 (A) and CYP3A4 (B) protein levels in 13 human liver microsomes. Correlation coefficients (r^2) obtained in these cases are shown.

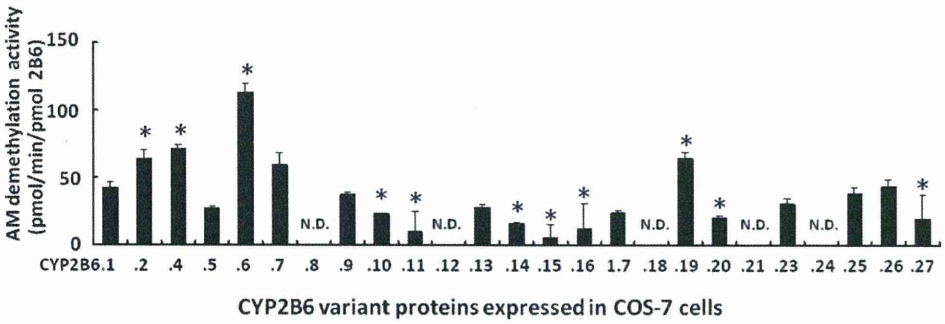

FIG. 6. AM demethylation activity of CYP2B6 proteins expressed in COS-7 cells. The concentration of AM was 50 μM. Each number corresponds to CYP2B6 variant proteins. Results are presented as the mean ± S.D. in triplicate. *, $P < 0.05$ compared with CYP2B6.1. N.D., not detectable.

has the highest intrinsic activity for AM demethylation, followed by CYP3A4. In the kinetic parameter analysis, the affinity of CYP2B6 was 4-fold higher than that of CYP3A4, and the V_{max}/apparent K_m of CYP2B6 was 6-fold higher than that of CYP3A4. These results suggest that AM demethylation is likely to be mainly catalyzed by CYP2B6 in the liver. The contribution of CYP2B6 to AM demethylation by human liver microsomes was further substantiated by showing a correlation to CYP2B6 protein content ($r^2 = 0.548$). However, van Agtmael et al. (1999b,c) have reported that administration of AM with grapefruit juice, a CYP3A4 inhibitor, increased the blood concentration of AM and DHA but not their elimination half-life. Thus, CYP3A4 in the small intestine might also play an important role in the metabolism of AM.

CYP2B6 is a genetically polymorphic enzyme (Zanger et al., 2007; Arenaz et al., 2010). In vitro functional characterization of polymorphically expressed CYP2B6 variants revealed that CYP2B6.4 and CYP2B6.6 increased AM demethylation activity, whereas CYP2B6.8, CYP2B6.11, CYP2B6.12, CYP2B6.14, CYP2B6.15, CYP2B6.16, CYP2B6.18, CYP2B6.20, CYP2B6.21, CYP2B6.24, and CYP2B6.27 exhibited no activity or decreased activity. These alterations were consistent with those of previous in vitro studies performed using bupropion, 7-ethoxy-4-trifluoromethylcoumarin, and selegiline as CYP2B6 substrates (Lang et al., 2004; Klein et al., 2005; Wang et al., 2006; Rotger et al., 2007; Watanabe et al., 2010). However, CYP2B6.2 exhibited increased AM demethylation activity, and the activity of CYP2B6.13 was similar to that of wild-type CYP2B6.1. There have been several reports that CYP2B6.2 exhibited no functional differences compared with CYP2B6.1 (Jinno et al., 2003; Watanabe et al., 2010) and that CYP2B6.13 had no metabolic activity toward 7-ethoxy-4-trifluoromethylcoumarin and selegiline (Watanabe et al., 2010). These results suggest that these CYP2B6 variants show substrate-dependent changes in the catalytic properties of the enzyme.

Gay et al. (2010) recently determined the crystal structure of CYP2B6, allowing the prediction of precise locations within the three-dimensional structure at which amino acid substitutions occur. They suggested that the K262R substitution on the G/H loop is assembled into a hydrogen-bonding network with His252, Thr255, Asp263, and Asp266 and is involved in protein stability. In this study, the AM demethylation activities of CYP2B6.12 (G99E) and CYP2B6.24 (Q476D) were not detectable. In the CYP2B6 protein structure, the Gly99 and Gln476 residues are located in substrate recognition site 1 and 6, respectively. These amino acid changes may reduce the affinity of CYP2B6 for AM. However, a number of amino acids with altered AM demethylation activity are located far from substrate recognition sites. Indeed, the apparent K_m values of AM demethylation were not significantly different among the CYP2B6 variants (Table 1). We hypothesize that the functional effects of these variants are transduced via long-range hydrogen-bonding networks or through subtle differences in the placement of secondary structural elements. In addition, most of the amino acid substitutions that abolished enzymatic activity are conserved among human P450s and are therefore critical for CYP2B6 activity.

This is the first study to functionally analyze CYP2B6 genetic variants with respect to AM demethylation activity. If CYP2B6 has a significant role in the metabolism of AM in vivo as well as in vitro, individuals with poor CYP2B6 metabolism might have higher plasma

TABLE 1

Kinetic parameters of AM demethylation by CYP2B6 proteins expressed in COS-7 cells

Results represent the mean ± S.D. of triplicate determinations.

Variants	Apparent K_m	V_{max}	V_{max}/Apparent K_m	V_{max}/Apparent K_m Ratio
	μM	$pmol \cdot min^{-1} \cdot pmol\ CYP2B6^{-1}$	$\mu l \cdot min^{-1} \cdot pmol\ CYP2B6^{-1}$	% *CYP2B6.1*
CYP2B6.1	3.10 ± 1.1	36.0 ± 5.67	12.4 ± 4.11	
CYP2B6.2	4.29 ± 2.7	64.4 ± 3.92*	18.8 ± 9.19	129
CYP2B6.4	2.73 ± 0.45	70.6 ± 9.29*	26.0 ± 2.42	223
CYP2B6.5	6.87 ± 6.8	19.8 ± 3.06	8.91 ± 11.3	24.8
CYP2B6.6	6.72 ± 3.0	150 ± 15.9*	24.2 ± 6.84	192
CYP2B6.7	2.80 ± 1.4	50.1 ± 12.3	19.2 ± 4.65	154
CYP2B6.9	4.44 ± 1.7	33.1 ± 5.20	8.38 ± 3.94	64.2
CYP2B6.10	1.93 ± 0.68	17.0 ± 5.03	9.98 ± 5.05	75.7
CYP2B6.13	7.33 ± 4.1	18.2 ± 5.54	2.93 ± 1.73	21.3
CYP2B6.14	5.06 ± 5.8	7.06 ± 1.63*	6.70 ± 9.40	12.0
CYP2B6.17	2.17 ± 0.40	21.2 ± 4.73	9.44 ± 2.45	84.0
CYP2B6.19	8.06 ± 8.9	36.9 ± 21.9	7.38 ± 6.15	39.4
CYP2B6.20	6.47 ± 9.8	9.85 ± 2.22*	8.79 ± 7.22	13.1
CYP2B6.23	1.91 ± 0.72	31.4 ± 7.71	17.6 ± 5.93	142
CYP2B6.25	2.04 ± 1.9	25.7 ± 7.31	21.6 ± 15.7	108
CYP2B6.26	5.50 ± 3.4	37.3 ± 6.04	10.1 ± 8.13	58.4
CYP2B6.27	4.50 ± 0.98	10.6 ± 6.16*	2.59 ± 1.82	20.2

* $P < 0.05$ compared with CYP2B6.1.